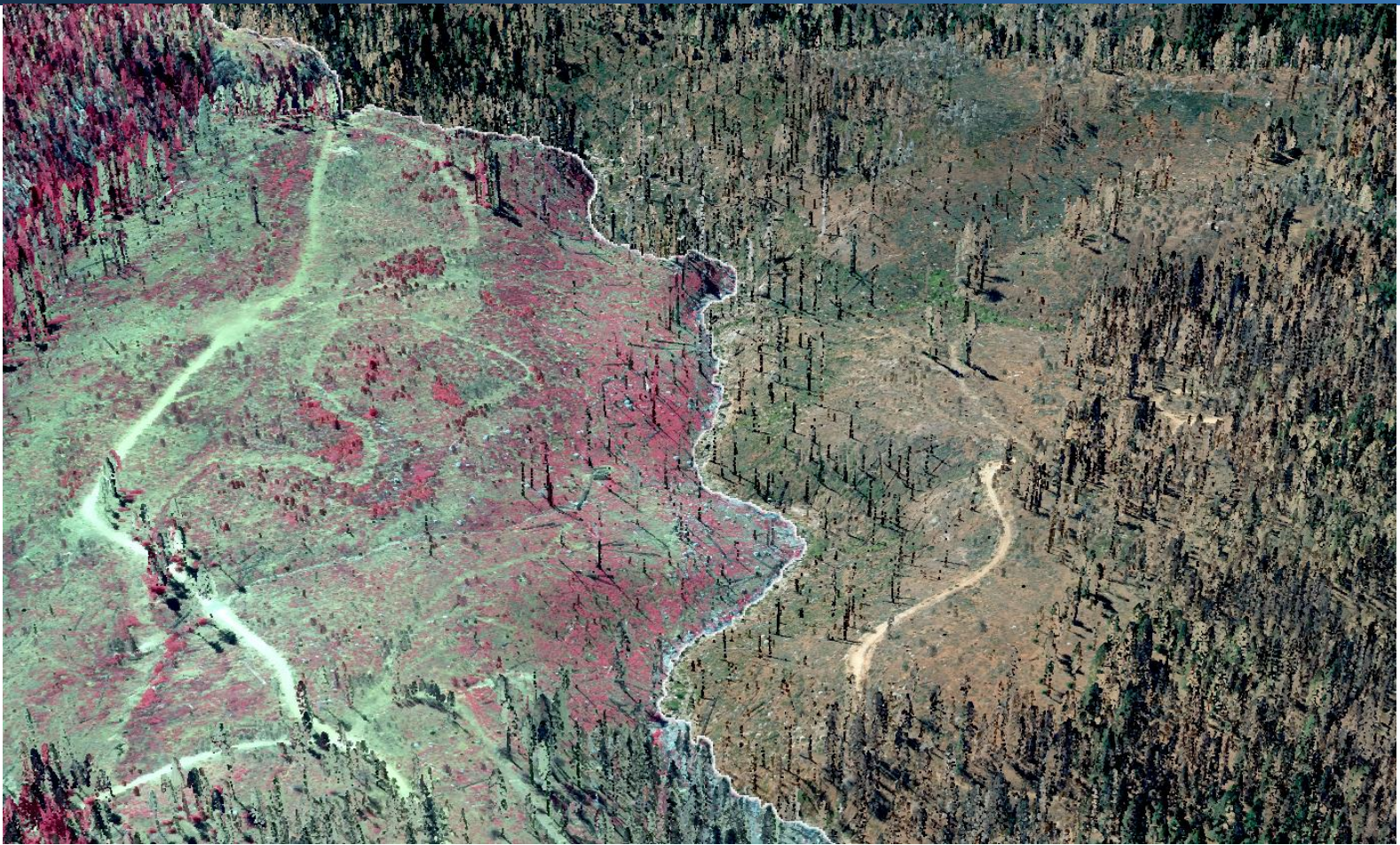




Applied  
Remote Sensing  
and Analysis

October 18, 2013



# Lassen & Plumas National Forests

## LiDAR Technical Data Report



**Susan Wilcox**  
USDA Forest Service  
PSW Station  
3644 Avtech Parkway  
Redding, CA  
PH: 530.252.5808



WSI Corvallis Office  
517 SW 2nd St., Suite 400  
Corvallis, OR 97333  
PH: 541-752-1204



# TABLE OF CONTENTS

INTRODUCTION .....	1
ACQUISITION .....	4
Planning.....	4
Ground Survey.....	5
Monumentation .....	5
RTK Surveys.....	6
Aerial Targets.....	7
Airborne Survey.....	8
LiDAR.....	8
Digital Imagery.....	9
PROCESSING .....	10
LiDAR Data .....	10
Intensity Normalization .....	12
Full Waveform Data Collection .....	13
Overview .....	13
Data Use and Applications.....	13
Digital Imagery .....	15
RESULTS & DISCUSSION .....	16
LiDAR Density .....	16
LiDAR Accuracy Assessments .....	20
LiDAR Absolute Accuracy .....	20
LiDAR Vertical Relative Accuracy .....	21
Digital Imagery Accuracy Assessment .....	22
CERTIFICATIONS .....	25
SELECTED IMAGES.....	26
APPENDIX A – POINT DENSITIES.....	29
APPENDIX B – ABSOLUTE ACCURACY .....	31
APPENDIX C – RELATIVE ACCURACY .....	32
APPENDIX D – CORS REFERENCE.....	33
GLOSSARY .....	34
ACCURACY CONTROLS .....	35

**Cover Photo:** View looking north at a recently burned section of Grizzly Creek near Middle Campsite in the Lassen National Forest. Image created from the LiDAR point cloud with RGB values assigned with NIR imagery (left) and true-color orthoimagery (right).





## INTRODUCTION

View of survey equipment in a burned area of the project showing the mountainous terrain in various successional stages of regrowth after exposure to wildfire.



In June 2013, WSI (Watershed Sciences, Inc.) was contracted by the USDA Forest Service – Region 5 to collect Light Detection and Ranging (LiDAR) data and digital imagery in the fall of 2013 for two areas of interest (AOIs) in the Lassen & Plumas National Forests in California: the Moonlight AOI in the Plumas NF and the Creeks, Grizzly, Storrie (CGS) AOI in the Lassen NF. Data were collected to aid the USFS in assessing the topographic and geophysical properties of the study area to support planning and development for fire rehabilitation and restoration efforts.

This report accompanies the delivered LiDAR data and imagery and documents data acquisition procedures, processing methods, and results of all accuracy assessments. Project specifics are shown in Table 1, the project extent can be seen in Figure 1, and a complete list of contracted deliverables provided to the USFS can be found in Table 2.

**Table 1: Acquisition dates, acreages, and data types collected for the Lassen & Plumas National Forests**

Project AOI	Contracted Acres	Buffered Acres	Acquisition Dates	Data Type
Moonlight, Plumas NF	123,809	128,141	Aug 3-9, 2013 Aug 13-15, 2013	LiDAR Only
Creeks, Grizzly, and Storrie, Lassen NF	61,448	64,872	July 30-31, 2013 Aug 3-6, 2013	LiDAR
			July 31, 2013 Aug 11, 2013	4 band (RGB, NIR) Digital Imagery

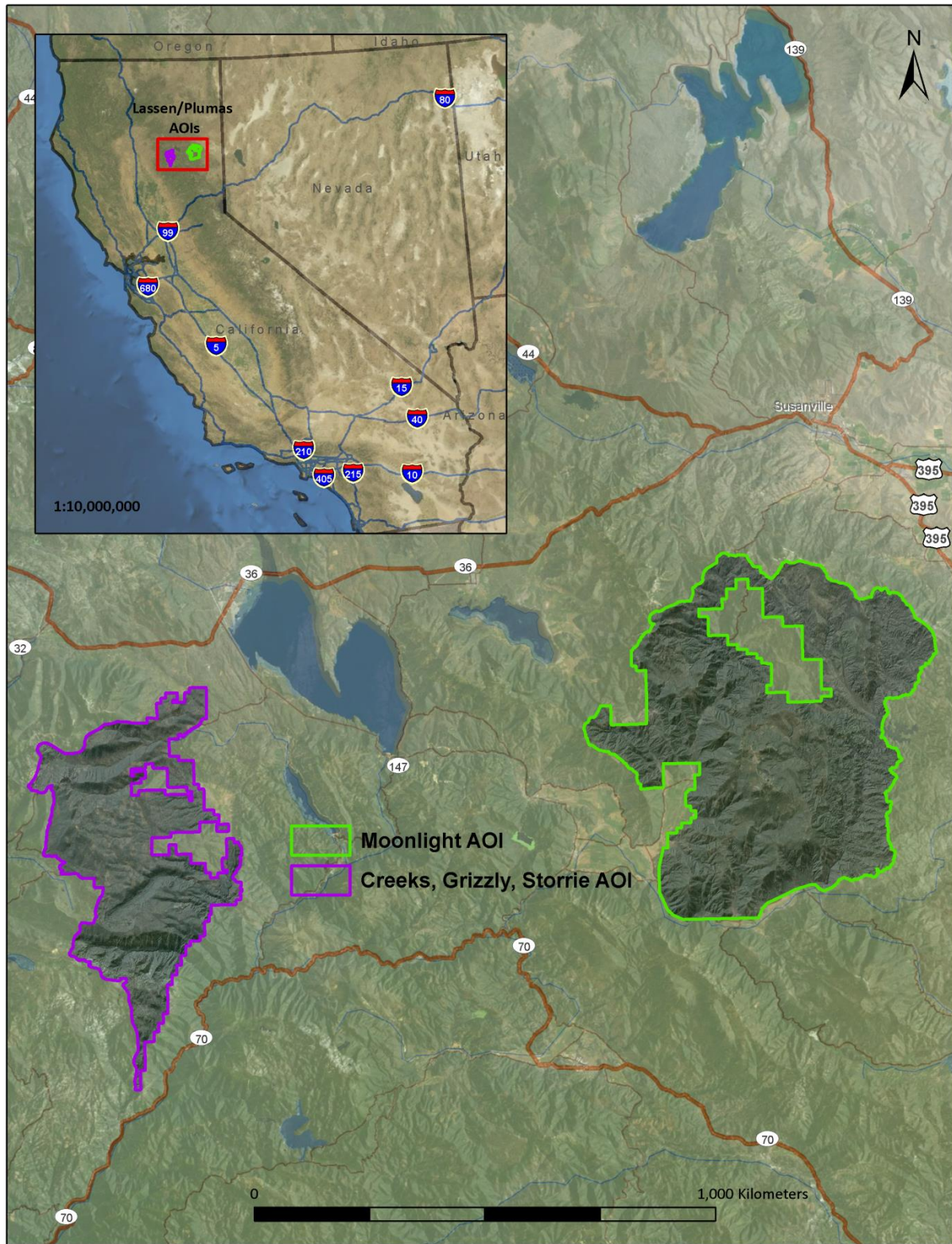


**Figure 1: Location map of the Lassen & Plumas National Forests project site in California**

**Table 2: Products delivered to the USDA Forest Service for the project area**

Lassen & Plumas National Forests <b>Products</b> <b>Projection: UTM Zone 10 North</b> <b>Horizontal Datum: NAD83 (CORS96)</b> <b>Vertical Datum: NAVD88 (GEOID03)</b> <b>Units: Meters</b>	
<b>LAS Files</b>	LAS v 1.2 <ul style="list-style-type: none"> <li>• All Returns</li> <li>• Ground Points</li> </ul> LAS v 1.3 <ul style="list-style-type: none"> <li>• All returns (full waveform – CGS only)</li> </ul>
<b>LiDAR Rasters</b>	1 Meter ESRI Grids <ul style="list-style-type: none"> <li>• Bare Earth Model</li> <li>• Highest Hit Model</li> </ul> 1 Meter GeoTiffs <ul style="list-style-type: none"> <li>• Normalized Intensity Images</li> </ul>
<b>Vectors</b>	Shapefiles (*.shp) <ul style="list-style-type: none"> <li>• Site Boundary</li> <li>• LiDAR Index</li> <li>• DEM/DSM Index</li> <li>• Orthoimagery Index</li> <li>• Smooth Best Estimate Trajectory (SBETs)</li> <li>• Flightline and Flightline Swath Shapefiles</li> </ul>
<b>Digital Imagery (CGS AOI only)</b>	Photo Block File Rasters: 30 centimeter pixel size <ul style="list-style-type: none"> <li>• Raw Image Frames (TIFF)</li> <li>• Orthorectified Frames (TIFF)</li> <li>• 4-band Orthorectified Imagery Mosaics (GeoTiff and MrSID compression)</li> </ul>



WSI Cessna Caravan



## Planning

In preparation for data collection WSI reviewed the project area using Google Earth and flightlines were developed using a combination of specialized software. Careful planning by acquisition staff entailed adapting the pulse rate, flight altitude, scan angle, and ground speed to ensure complete coverage of the LiDAR study area at the target point density of  $\geq 8$  pulses per square meter. Efforts are taken to optimize flight paths by minimizing flight times while meeting all accuracy specifications.

Factors such as satellite constellation availability and weather windows must be considered during the planning stage. Any weather hazards or conditions affecting the flight were continuously monitored due to their potential impact on the daily success of airborne and ground operations. In addition, a variety of logistical considerations required review including survey site access, potential air space restrictions, and availability of company resources (both staff and equipment).



## Ground Survey

Ground survey data are used to geospatially correct the aircraft positional coordinate data and to perform quality assurance checks on final LiDAR data and orthoimagery products. Ground surveys, including monumentation and ground check points, are conducted to support the airborne acquisition process.



## Monumentation

The spatial configuration of ground survey monuments provided redundant control within 13 nautical miles of the mission areas for LiDAR flights. Monuments were also used for collection of ground control points using RTK survey techniques (see **RTK** below).

Monument locations were selected with consideration for satellite visibility, field crew safety, and optimal location for RTK coverage. WSI utilized one existing monument and established 15 new monuments (Table 3, Figure 2). New monumentation was set using 5/8"x30" rebar topped with stamped 2" aluminum caps. WSI's professional land surveyor, Chris Yotter-Brown (ORPLS#60438LS) oversaw the establishment of all monuments.

**Table 3: Monuments established for the project acquisition. Coordinates are on the NAD83 (CORS96) datum, epoch 2002.00**

Monument ID	Latitude	Longitude	Ellipsoid (meters)
LA_SF_EG2	40° 08' 34.70380"	-121° 15' 12.98245"	1291.696
LAS_01	40° 05' 12.48085"	-121° 22' 19.38632"	1931.549
LAS_02	40° 04' 16.24621"	-120° 39' 47.71887"	1227.504
LAS_03	40° 09' 55.56534"	-120° 43' 48.50061"	2165.031
LAS_04	40° 10' 30.86058"	-120° 36' 19.08785"	1552.091
LAS_05	40° 13' 47.71091"	-120° 39' 20.37562"	1656.390
LAS_06	40° 14' 43.62613"	-120° 46' 30.12424"	1556.660
LAS_07	40° 12' 52.89756"	-121° 16' 38.15522"	1414.394
LAS_08	40° 04' 31.31931"	-121° 15' 12.40753"	1270.153
LAS_09	40° 10' 29.05343"	-121° 24' 36.19102"	1678.591
LAS_10	40° 17' 57.77070"	-120° 40' 26.31486"	2102.417
LAS_11	40° 01' 28.16739"	-121° 25' 01.17413"	1880.793
LAS_12	40° 10' 04.16239"	-120° 47' 07.20317"	1162.175
LAS_13	40° 11' 12.75901"	-120° 49' 28.83632"	1604.402
LAS_14	40° 13' 50.38006"	-120° 49' 54.06461"	1691.221
LAS_15	40° 15' 09.64462"	-120° 39' 06.36448"	1821.060

To correct the continuous onboard measurements of the aircraft position recorded throughout the missions, WSI concurrently conducted multiple static Global Navigation Satellite System (GNSS) ground surveys (1 Hz recording frequency) over each monument. After the airborne survey, the static GPS data were triangulated with nearby Continuously Operating Reference Stations (CORS) using the Online Positioning User Service (OPUS<sup>1</sup>) for precise positioning. Multiple independent sessions over the same monument were processed to confirm antenna height measurements and to refine position accuracy.

See Appendix D for a description of the CORS network used to establish monument positions.

## RTK Surveys

For the real time kinematic (RTK) check point data collection, a Trimble R7 base unit was positioned at a nearby monument to broadcast a kinematic correction to a roving Trimble R8 or R10 GNSS receiver. All RTK measurements were made during periods with a Position Dilution of Precision (PDOP) of  $\leq 3.0$  with at least six satellites in view of the stationary and roving receivers. When collecting RTK data, the rover would record data while stationary for five seconds, then calculate the pseudorange position using at least three one-second epochs. Relative errors for the position must be less than 1.5 cm horizontal and 2.0 cm vertical in order to be accepted. See Table 4 for Trimble unit specifications.

RTK positions were collected on paved roads and other hard surface locations such as gravel or stable dirt roads that also had good satellite visibility. RTK measurements were not taken on highly reflective surfaces such as center line stripes or lane markings on roads due to the increased noise seen in the laser returns over these surfaces. The distribution of RTK points depended on ground access constraints and may not be equitably distributed throughout the study area. See Figure 2 for the distribution of RTK in this project.

**Table 4: Trimble equipment identification**

Receiver Model	Antenna	OPUS Antenna ID	Use
Trimble R7 GNSS	Zephyr GNSS Geodetic Model 2 RoHS	TRM57971.00	Static
Trimble R8	Integrated Antenna R8 Model 2	TRM_R8_GNSS	RTK
Trimble R10	Integrated Antenna R10	TRMR10	RTK

<sup>1</sup> OPUS is a free service provided by the National Geodetic Survey to process corrected monument positions.  
<http://www.ngs.noaa.gov/OPUS>.

## Aerial Targets

Aerial targets were placed throughout the project area prior to imagery acquisition in order to geo-spatially correct the orthoimagery. Located within RTK range of the ground survey monuments, the targets were secured with surveyor's nails and routinely checked for disturbance (Figure 2).

The air targets used for the Lassen & Plumas National Forests project were white and black vinyl squares approximately 115 cm in size. Each target was precisely located using five RTK points (four corner points and a center point). Other orthophoto control included permanent road stripes and painted crosses on asphalt pavement.

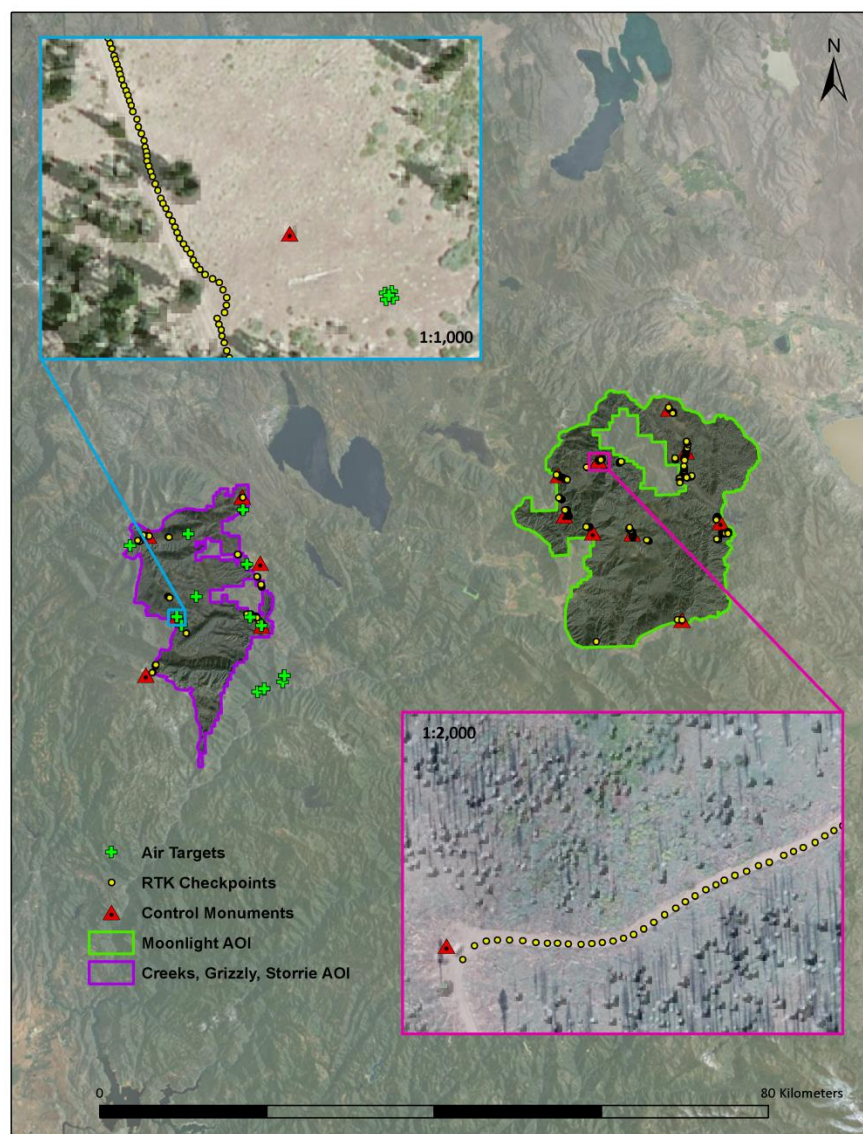


Figure 2: Basestation, aerial target, and RTK checkpoint location map



# Airborne Survey

## LiDAR

The LiDAR survey was accomplished with a Leica ALS50 Phase II and ALS60 systems independently mounted in two Cessna Caravans. Table 5 summarizes the settings used to yield an average pulse density of  $\geq 8$  pulses/m<sup>2</sup> over the Lassen & Plumas National Forests terrain. It is not uncommon for some types of surfaces (e.g. dense vegetation or water) to return fewer pulses to the LiDAR sensor than the laser originally emitted. These discrepancies between native and delivered density will vary depending on terrain, land cover, and the prevalence of water bodies.

**Table 5: LiDAR specifications and survey settings**

LiDAR Survey Settings & Specifications	
Sensor	Leica ALS50 and ALS60
Survey Altitude (AGL)	900 m
Target Pulse Rate	85-107.8 kHz
Sensor Configuration	Single Pulse in Air (SPiA)
Laser Pulse Diameter	21 cm
Field of View	28°
GPS Baselines	$\leq 13$ nm
GPS PDOP	$\leq 3.0$
GPS Satellite Constellation	$\geq 6$
Maximum Returns	4
Intensity	8-bit
Resolution/Density	Average 8 pulses/m <sup>2</sup>
Accuracy	RMSE <sub>z</sub> $\leq 15$ cm

**Leica ALS60 LiDAR sensor**



To reduce laser shadowing and increase surface laser painting, all areas were surveyed with an opposing flight line side-lap of  $\geq 50\%$  ( $\geq 100\%$  overlap). The Leica laser systems record up to four range measurements (returns) per pulse. All discernible laser returns were processed for the output dataset.

To accurately solve for laser point position (geographic coordinates x, y, z), the positional coordinates of the airborne sensor and the attitude of the aircraft were recorded continuously throughout the LiDAR data collection mission. Position of the aircraft was measured twice per second (2 Hz) by an onboard differential GPS unit. Aircraft attitude was measured 200 times per second (200 Hz) as pitch, roll, and yaw (heading) from an onboard inertial measurement unit (IMU). To allow for post-processing correction and calibration, aircraft/sensor position and attitude data are indexed by GPS time.

## Digital Imagery

The aerial imagery for the CGS AOI was collected using an UltraCam Eagle 260 megapixel digital camera (Table 6) mounted in a Cessna Caravan. The UltraCam Eagle is a large format digital aerial camera manufactured by Microsoft Corporation. The system is gyro-stabilized and simultaneously collects panchromatic and multispectral (RGB, NIR) imagery. Panchromatic lenses collect high resolution imagery by illuminating 9 charge coupled device (CCD) arrays, writing 9 raw image files. RGB and NIR lenses collect lower resolution imagery, written as 4 individual raw image files. Level 2 images are created by stitching together raw image data from the 9 panchromatic CCDs and are ultimately combined with the multispectral image data to yield Level 3 pan-sharpened TIFFs.

**Table 6: Camera manufacturer's specifications**

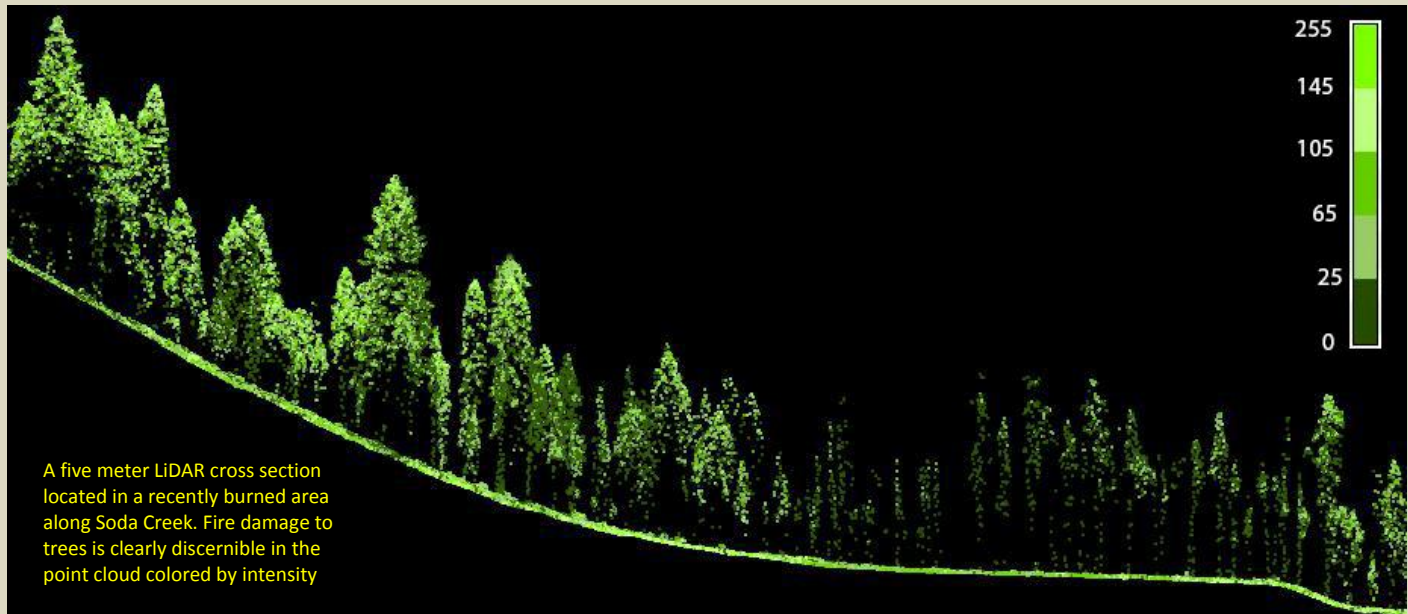
UltraCam Eagle	
<b>Focal Length</b>	80 mm
<b>Data Format</b>	RGB NIR
<b>Pixel Size</b>	5.2 $\mu$ m
<b>Image Size</b>	20,010 x 13,080 pixels
<b>Frame Rate</b>	1.8 seconds
<b>FOV</b>	66° x 46°



For the CGS AOI, images were collected in 4 spectral bands (red, green, blue, and NIR) with 60% along track overlap and 30% sidelap between frames. The acquisition flight parameters were designed to yield a native pixel resolution of 30cm. The resulting spatial accuracies (RMSE) were routinely  $\leq 45$ cm at 95% confidence level. Orthophoto specifications particular to the project are shown in Table 7.

**Table 7: Project-specific orthophoto specifications**

Digital Orthophotography Specifications	
<b>Equipment</b>	UltraCam Eagle
<b>Spectral Bands</b>	Red, Green, Blue, NIR
<b>Resolution</b>	30 cm pixel size
<b>Along Track Overlap</b>	$\geq 60\%$
<b>Flight Altitude (MSL)</b>	5,700 meters
<b>GPS Baselines</b>	$\leq 25$ nm
<b>GPS PDOP</b>	$\leq 3.0$
<b>GPS Satellite Constellation</b>	$\geq 6$
<b>Horizontal Accuracy</b>	0.35 m
<b>Image</b>	8-bit GeoTiff



## LiDAR Data

Upon the LiDAR data's arrival to the office, WSI processing staff initiates a suite of automated and manual techniques to process the data into the requested deliverables. Processing tasks include GPS control computations, smoothed best estimate trajectory (SBET) calculations, kinematic corrections, calculation of laser point position, calibration for optimal relative and absolute accuracy, and classification of ground and non-ground points (Table 8). Processing methodologies were tailored for the steep slopes and rocky outcrops of the Lassen-Plumas landscape and the intended wildfire restoration application of the point data. A full description of these tasks can be found in Table 9.

**Table 8: ASPRS LAS classification standards applied to the Lassen & Plumas National Forests dataset**

Classification Number	Classification Name	Classification Description
1	Default/ Unclassified	Laser returns that are not included in the ground class and not dismissed as Noise or Withheld points
2	Ground	Ground that is determined by a number of automated and manual cleaning algorithms to determine the best ground model the data can support
7	Noise	Laser returns that are often associated with birds or artificial points below the ground surface also known as "pits".
11	Withheld	Laser returns that have intensity values of 0 or 255 before normalization.



**Table 9: LiDAR processing workflow**

LiDAR Processing Step	Software Used
Resolve kinematic corrections for aircraft position data using kinematic aircraft GPS and static ground GPS data.	Waypoint GPS v.8.3 Trimble Business Center v.3.00 Geographic Calculator 2013
Develop a smoothed best estimate of trajectory (SBET) file that blends post-processed aircraft position with attitude data. Sensor head position and attitude are calculated throughout the survey. The SBET data are used extensively for laser point processing.	IPAS TC v.3.1
Calculate laser point position by associating SBET position to each laser point return time, scan angle, intensity, etc. Create raw laser point cloud data for the entire survey in *.las (ASPRS v. 1.2) format. Data are converted to orthometric elevations (NAVD88) by applying a Geoid12 correction.	ALS Post Processing Software v.2.74
Import raw laser points into manageable blocks (less than 500 MB) to perform manual relative accuracy calibration and filter erroneous points. Ground points are then classified for individual flight lines (to be used for relative accuracy testing and calibration).	TerraScan v.13.008
Using ground classified points per each flight line, the relative accuracy is tested. Automated line-to-line calibrations are then performed for system attitude parameters (pitch, roll, heading), mirror flex (scale) and GPS/IMU drift. Calibrations are calculated on ground classified points from paired flight lines and results are applied to all points in a flight line. Every flight line is used for relative accuracy calibration.	TerraMatch v.13.002
Classify resulting data to ground and other client designated ASPRS classifications (Table 8). Assess statistical absolute accuracy via direct comparisons of ground classified points to ground RTK survey data.	TerraScan v.13.008 TerraModeler v.13.002
Generate bare earth models as triangulated surfaces. Highest hit models were created as a surface expression of all classified points (excluding the noise and withheld classes). All surface models were exported as ESRI grids at a 1 meter pixel resolution.	TerraScan v.13.008 ArcMap v. 10.1 TerraModeler v.13.002
Correct intensity values for variability and export intensity images as GeoTiffs at a 1 meter pixel resolution.	TerraScan v.13.008 ArcMap v. 10.1 TerraModeler v.13.002

## Intensity Normalization

Laser return intensity is a unitless measure of discrete return voltage, stored as an integer value from 0 to 255 (8-bit). Intensity values correspond to the reflectivity and composition of the target. Differences in the magnitude of intensity values across similar targets is a function of receiver auto gain control (AGC), atmospheric (transmissivity and target range), and the angle of incidence. These components influence intensity at different rates and magnitudes, with AGC comprising the majority of influence. The result is variability in returned intensity values across the landscape that can reduce the utility of these data for analysis. This variability represents sources of noise with respect to the radiometric accuracy of a laser return.

Variability in each of these components is minimized mathematically to arrive at a normalized intensity value that approaches a true radiometric value for each discrete LiDAR return. WSI employs proprietary software to normalize intensity values. Normalization is based on the assessment of the components discussed above to a reference gain value for the laser that was used for this project.

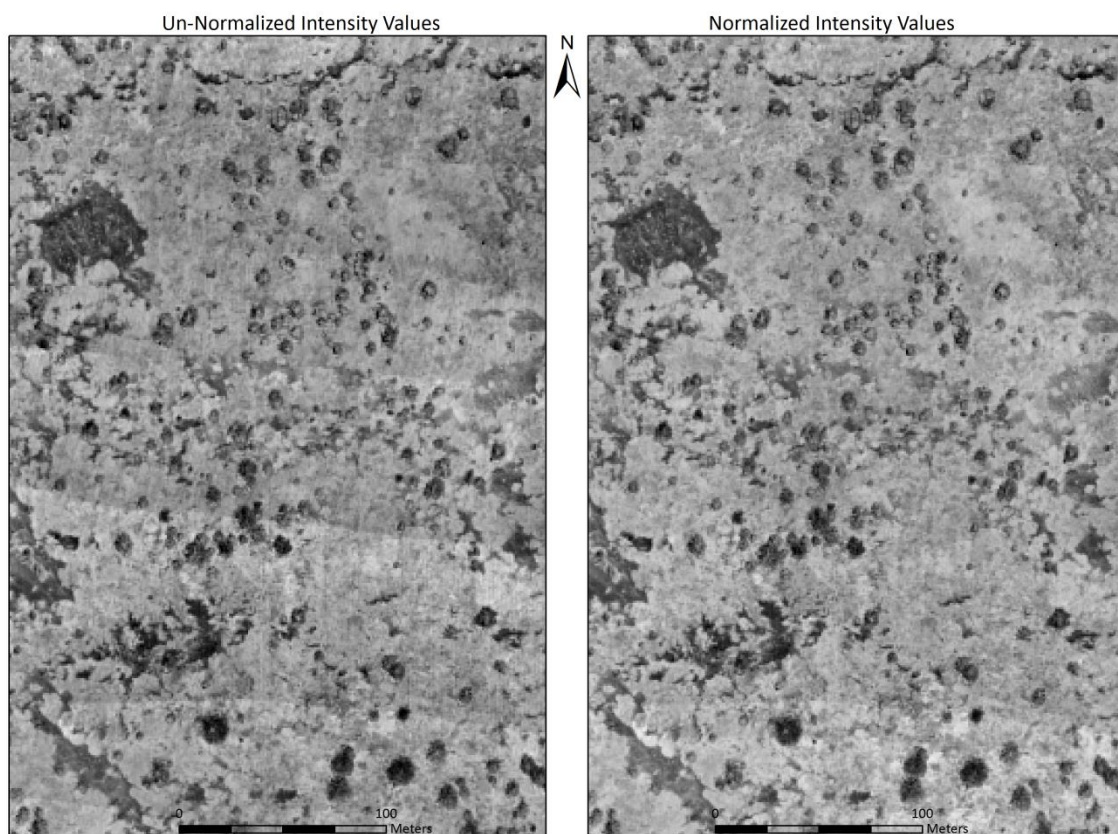


**Figure 3: Comparison of normalized and non-normalized intensities**

# Full Waveform Data Collection

## Overview

WSI collected full waveform Light Detection and Ranging data (LiDAR) of the Creeks, Grizzly, Storrie (CGS) AOI for the USDA Forest Service – Region 5 on July 30-31, 2013 and August 3-6, 2013 (Table 1, Figure 1). This data serves to complement the discrete return datasets for the Lassen National Forest study area offering a new resource for innovative approaches to forest resource applications. The LiDAR sensor (Leica ALS50-II) used on the flight was integrated with the Leica WDM65 Waveform Digitizer Module to capture the entire return signal (Table 10). Flight planning parameters were designed to yield full waveform digitization of every return pulse.

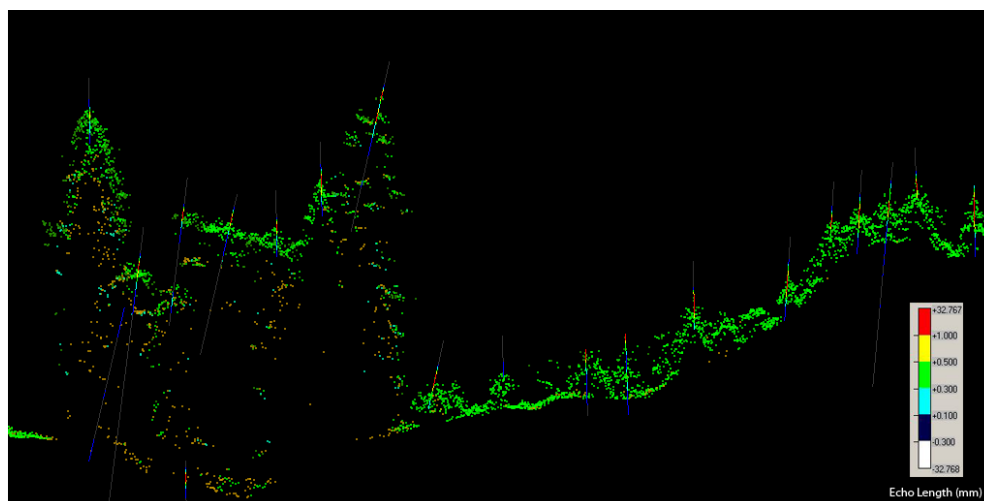
**Table 10: Full Waveform specifications for Lassen data collection**

Sensor	<i>Leica ALS50-ii</i>
Digitizer	<i>WDM65</i>
Sampling Routine	<i>256 Samples @ 2 nsec intervals</i>

## Data Use and Applications

Full-waveform LiDAR data has recently emerged as a prominent tool for forest resource applications. Rapid advances in onboard airborne data capture technology have allowed for the collection and storage of full-waveform LiDAR data, however, tools used to exploit the full capabilities of this information are in their infancy. WSI is currently developing software and methods to deliver waveform data (native and derived) in formats readily accessible by popular LiDAR software packages. The current deliverable format is LAS 1.3, but can be converted into other formats such as PulseWaves (Figure 4).

Supplied are the raw data files (LAS 1.3) needed to explore the waveforms of the LiDAR acquisition in the Microstation/TerraScan environment (or other compatible software). The calibrated \*.las (v1.2) files can be referenced to the waveform information contained in the \*.las(v1.3) by creating a link through the \*.trj files.





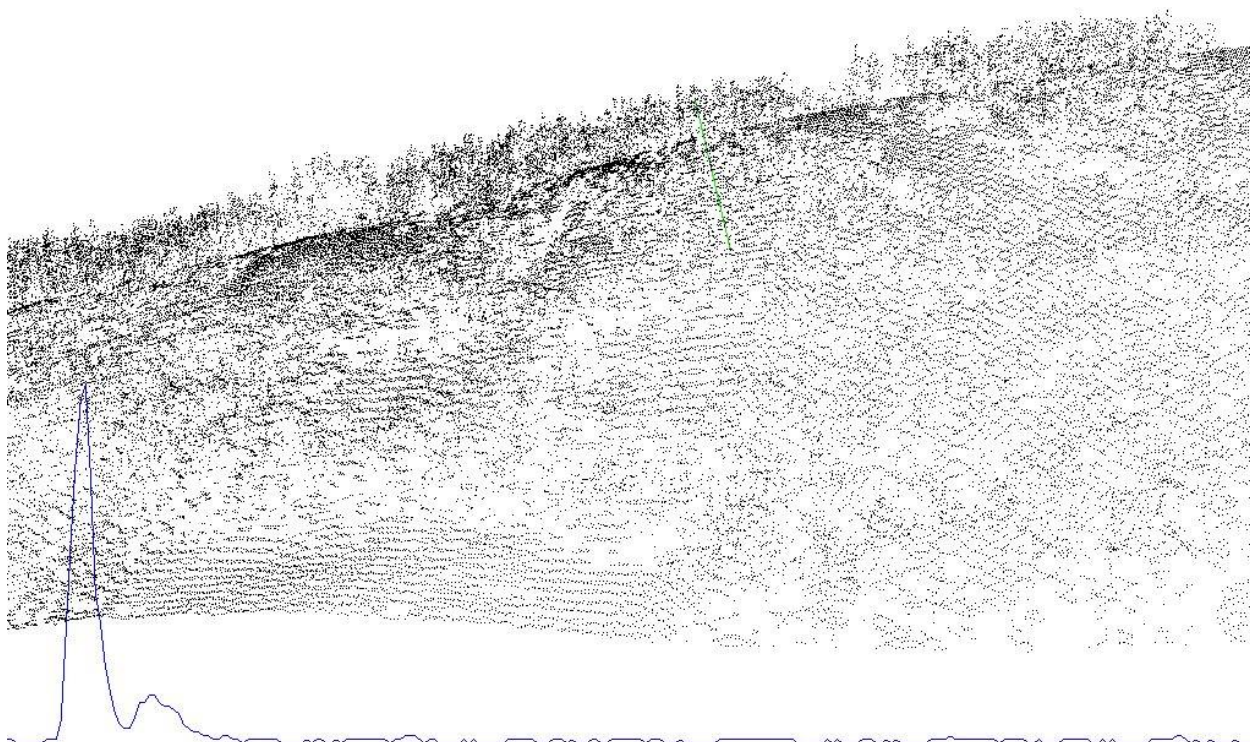


**Figure 4: Example of full waveform data from Lassen National Forest displayed in PulseWaves Viewer**

## Digital Imagery

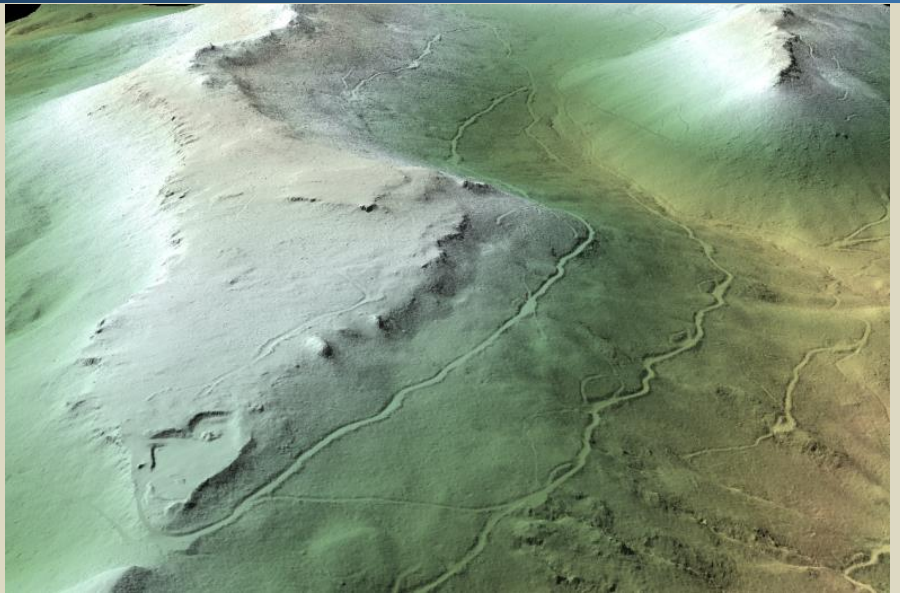
As with the LiDAR, the collected digital photographs went through multiple processing steps to create final orthophoto products. Initially, image radiometric values were calibrated to specific gain and exposure settings. Photo position and orientation were then calculated by linking the time of image capture to the smoothed best estimate of trajectory (SBET) file created during LiDAR post-processing. Within Leica Photogrammetry Suite (LPS), an automated aerial triangulation was performed to tie images together and adjust the photo block to align with ground control.

Adjusted images were orthorectified using the LiDAR-derived ground model to remove displacement effects from topographic relief inherent in the imagery and individual orthorectified TIFFs were blended together to remove seams. The final mosaics were corrected for any remaining radiometric differences between images using Inpho's OrthoVista. The processing workflow for orthophotos is summarized in Table 11.

**Table 11: Orthophoto processing workflow**

Orthophoto Processing Step	Software Used
Resolve GPS kinematic corrections for the aircraft position data using kinematic aircraft GPS (collected at 2HS) and static ground GPS (1Hz) data collected over geodetic controls.	POSPac MMS v. 6.1
Develop a smooth best estimate trajectory (SBET) file that blends post-processed aircraft position with attitude data. Sensor heading, position, and attitude are calculated throughout the survey.	POSPac MMS v. 5.4
Create an exterior orientation file (EO) for each photo image with omega, phi, and kappa.	POSPac MMS v. 6.1
Convert Level 00 raw imagery data into geometrically corrected Level 02 image files.	UltraMap 2.3.2
Apply radiometric adjustments to Level 02 image files to create Level 03 Pan-sharpened TIFFs.	UltraMap 2.3.2
Apply EO to photos, measure ground control points and perform aerial triangulation.	LPS 2013
Import DEM, orthorectify and clip triangulated photos to the specified area of interest.	LPS 2013
Mosaic orthorectified imagery, blending seams between individual photos and correcting for radiometric differences between photos.	Inpho v. 5.5

Bare earth image colored by elevation, looking north from Wildcat Ridge toward Diamond Mountains in the Plumas National Forest.



### LiDAR Density

The sensor is set to acquire a native density of 8 points/m<sup>2</sup>. Depending on the nature of the terrain, the first returned echo will be the highest hit surface. In vegetated areas, the first return surface will represent the top of the canopy, while in clearings or on paved roads, the first return surface will represent the ground. The ground density differs from the first return density due to the fact that in vegetated areas, fewer returns may penetrate the canopy. The ground classification is generally determined by first echo returns in non-vegetated areas combined with last echo returns in vegetated areas. The pulse density distribution will vary within the study area due to laser scan pattern and flight conditions. Additionally, some types of surfaces (i.e. breaks in terrain, water, steep slopes) may return fewer pulses to the sensor than originally emitted.

The cumulative average first-return density for the LiDAR data for the Lassen-Plumas study area was 11.05 points/m<sup>2</sup> while the average cumulative ground density was 2.10 points/m<sup>2</sup> (Table 12). The statistical distribution of first returns (Figure 5) and classified ground points (Figure 6) are portrayed below. Also presented are the spatial distribution of average first return densities (Figure 7) and ground point densities (Figure 8) for 100mx100m cells covering the project area. Frequency distributions by area of interest are shown in Appendix A.

**Table 12: Average LiDAR point densities**

Classification	Point Density		
AOI	Cumulative	Creeks, Grizzly & Storrie	Moonlight
First-Return	11.05 points/m <sup>2</sup>	10.86 points/m <sup>2</sup>	11.15 points/m <sup>2</sup>
Ground Classified	2.10 points/m <sup>2</sup>	1.96 points/m <sup>2</sup>	2.17 points/m <sup>2</sup>



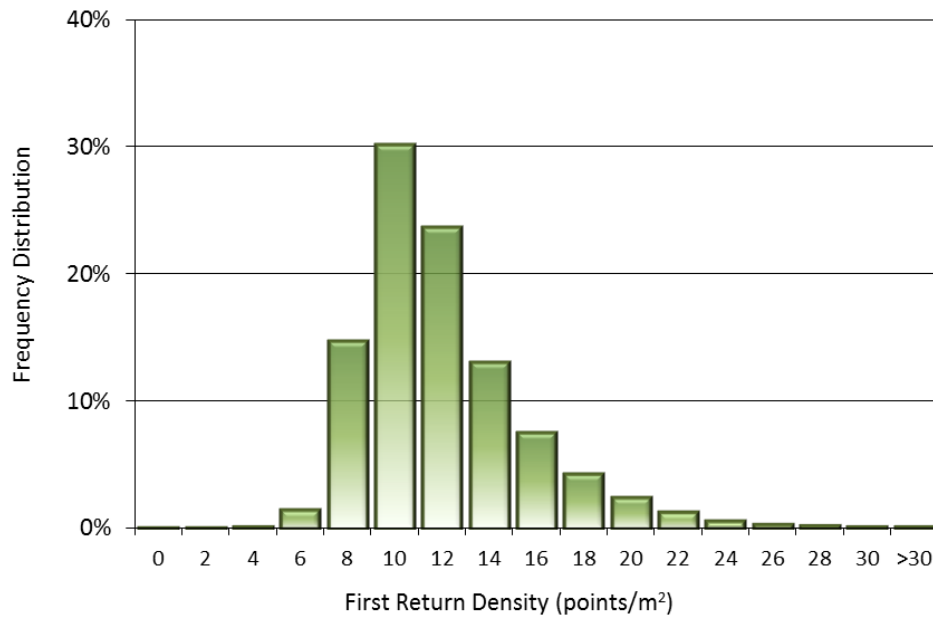


**Figure 5: Cumulative frequency distribution of first return densities (native densities) measured in 100mx100m cells**

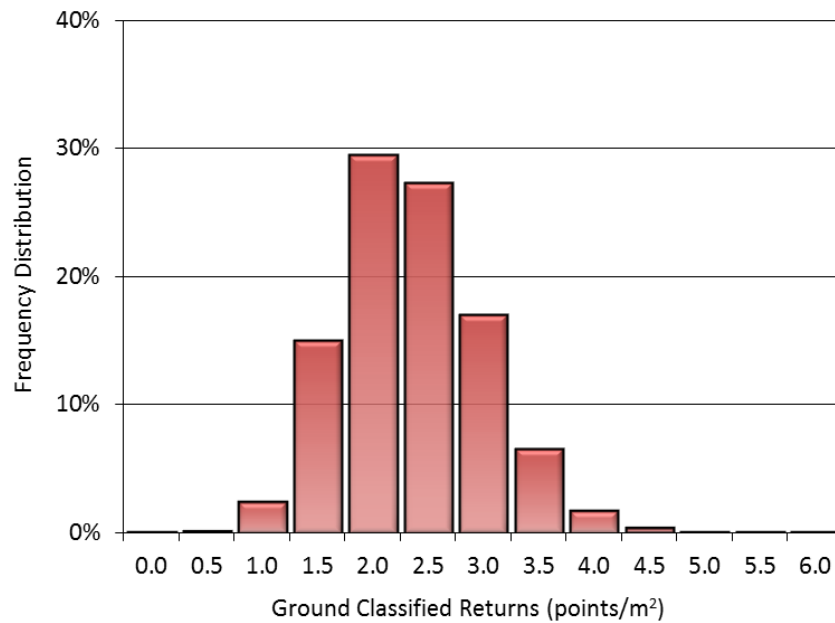


**Figure 6: Cumulative frequency distribution of ground return densities measured in 100mx100m cells**

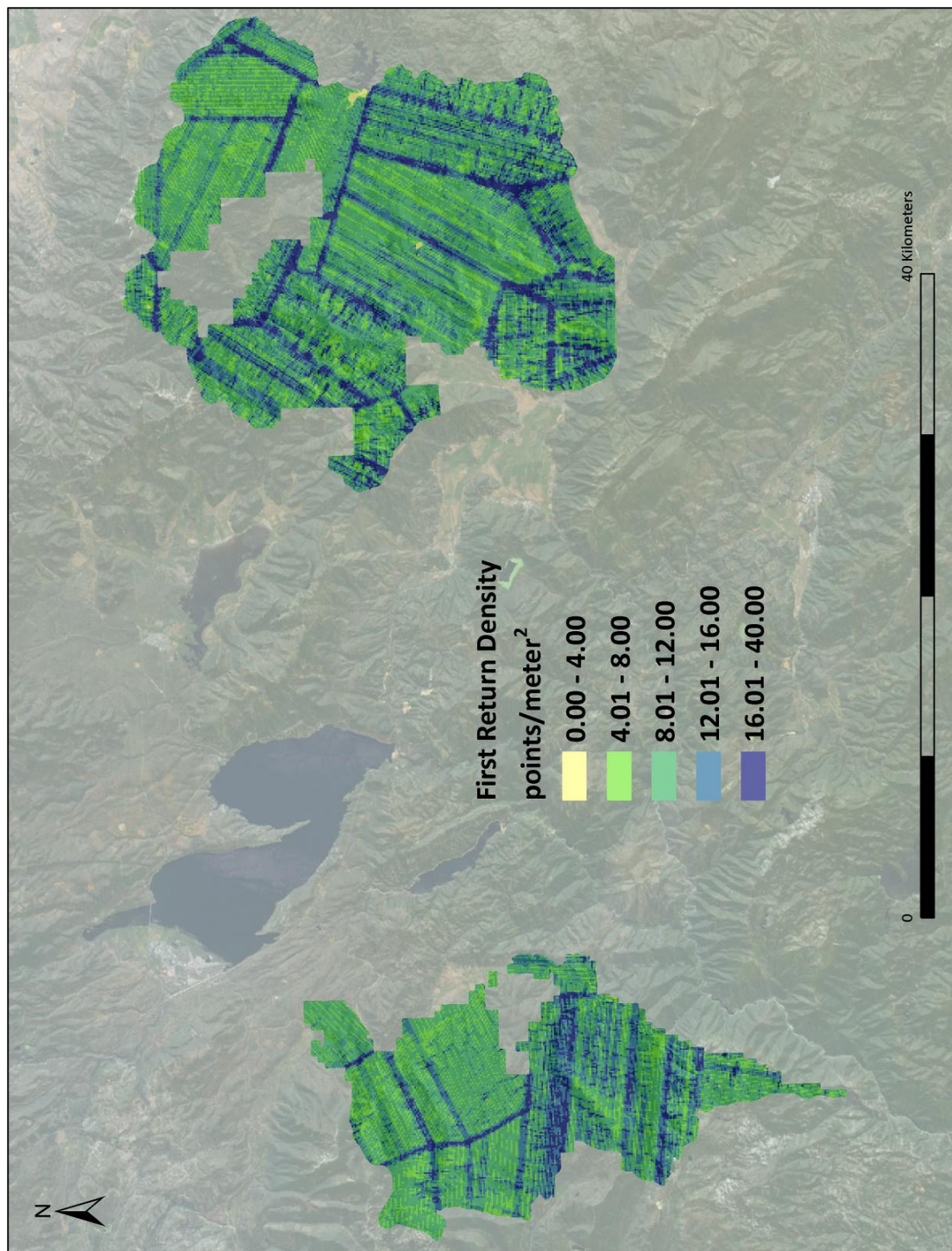


Figure 7: First return density map for the Lassen-Plumas site (100mx100m cells)



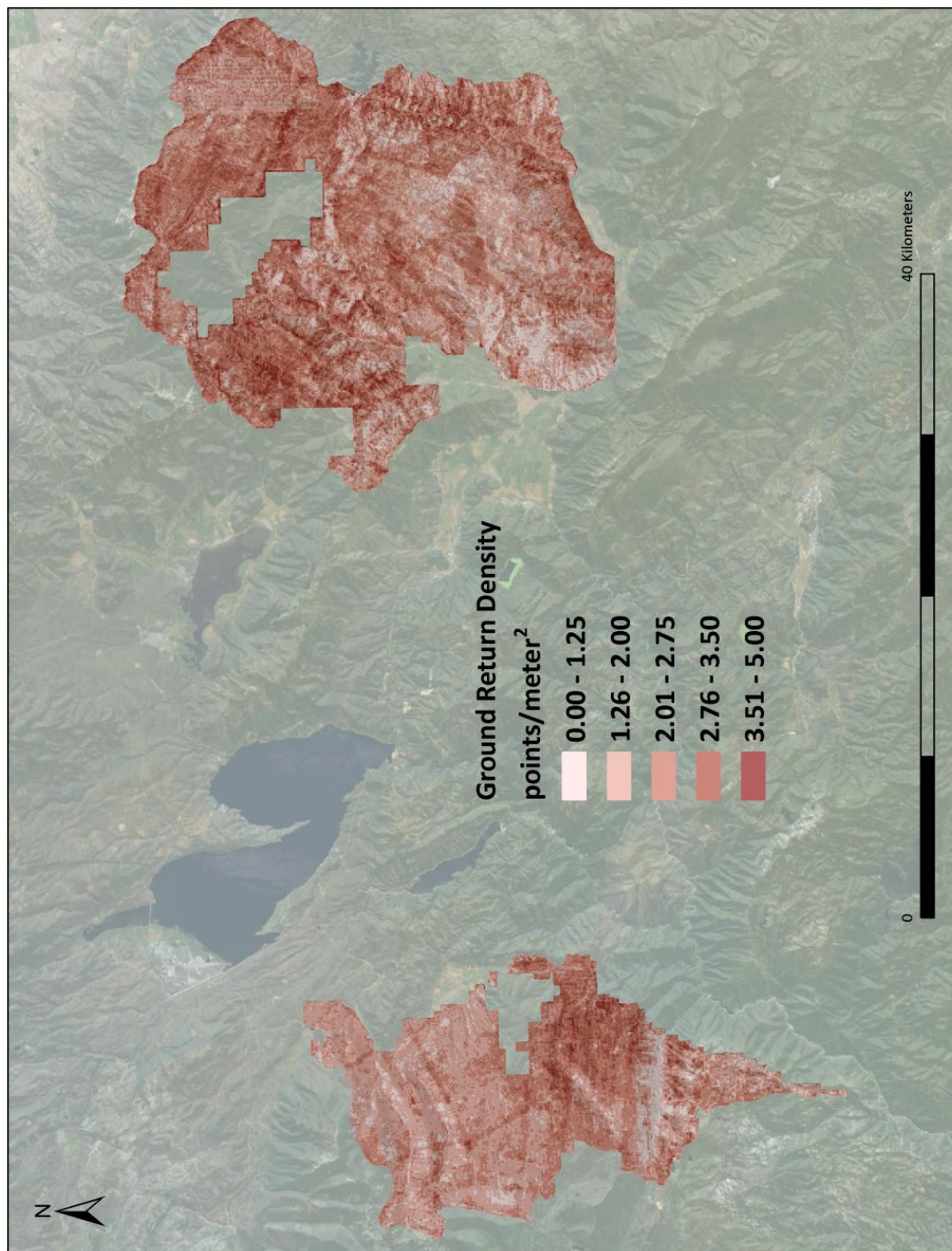


Figure 8: Ground density map for the Lassen-Plumas site (100mx100m cells)

## LiDAR Accuracy Assessments

The accuracy of the LiDAR data collection can be described in terms of absolute accuracy (the consistency of the data with external data sources) and relative accuracy (the consistency of the dataset with itself). Further information on sources of error and operational measures used to improve relative accuracy can be found in the Accuracy Controls section at the end of this document.

### LiDAR Absolute Accuracy

Vertical absolute accuracy was primarily assessed from RTK ground check point (GCP) data collected on open, bare earth surfaces with level slope ( $<20^\circ$ ). Fundamental Vertical Accuracy (FVA) reporting is designed to meet guidelines presented in the FGDC National Standard for Spatial Data Accuracy<sup>2</sup>. FVA compares known RTK ground survey check points to the triangulated ground surface generated by the LiDAR points. FVA is a measure of the accuracy of LiDAR point data in open areas where the LiDAR system has a “very high probability” of measuring the ground surface and is evaluated at the 95% confidence interval ( $1.96\sigma$ ).

Absolute accuracy is described as the mean and standard deviation (sigma  $\sigma$ ) of divergence of the ground surface model from ground survey point coordinates. These statistics assume the error for x, y, and z is normally distributed, and therefore the skew and kurtosis of distributions are also considered when evaluating error statistics. A total of 3,553 RTK points were collected across the project area resulting in an average cumulative absolute accuracy of 0.002 meters. (Table 13, Figure 9). Absolute accuracy histograms by area of interest are shown in Appendix B.

**Table 13: Absolute accuracy**

	Cumulative	Creeks, Grizzly & Storrie	Moonlight
<b>Sample</b>	3,553 points	1,524 points	2,029 points
<b>Average</b>	0.002 m	0.003 m	0.001 m
<b>Median</b>	0.003 m	0.004 m	0.002 m
<b>RMSE</b>	0.026 m	0.029 m	0.023 m
<b>Standard Deviation (<math>1\sigma</math>)</b>	0.026 m	0.029 m	0.023 m
<b><math>1.96\sigma</math></b>	0.050 m	0.057 m	0.045 m

---

<sup>2</sup> Federal Geographic Data Committee, Geospatial Positioning Accuracy Standards (FGDC-STD-007.3-1998). Part 3: National Standard for Spatial Data Accuracy. <http://www.fgdc.gov/standards/projects/FGDC-standards-projects/accuracy/part3/chapter3>



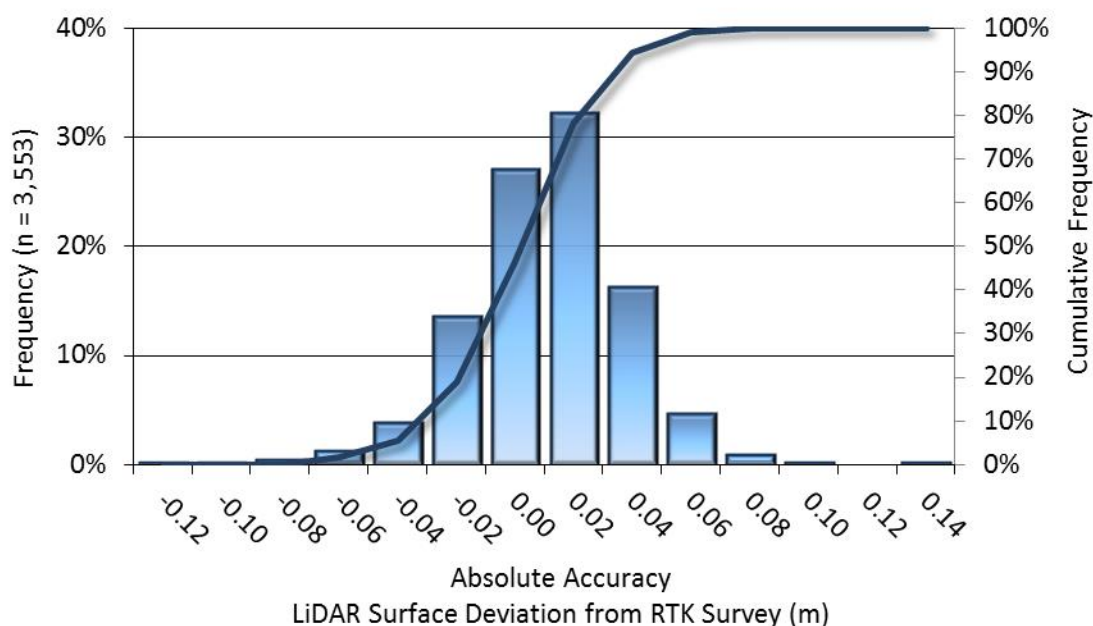


**Figure 9: Cumulative frequency histogram for LiDAR surface deviation from RTK values**

## LiDAR Vertical Relative Accuracy

Relative vertical accuracy refers to the internal consistency of the data set as a whole: the ability to place an object in the same location given multiple flight lines, GPS conditions, and aircraft attitudes. When the LiDAR system is well calibrated, the swath-to-swath vertical divergence is low (<0.10 meters). The relative vertical accuracy is computed by comparing the ground surface model of each individual flight line with its neighbors in overlapping regions. The cumulative average (mean) line to line relative vertical accuracy for the Lassen & Plumas National Forests study site was 0.047 meters. (Table 14, Figure 10). Relative accuracy histograms by area of interest are shown in Appendix C.

**Table 14: Relative accuracy**

	Cumulative	Creeks, Grizzly & Storrie	Moonlight
<b>Sample</b>	986 surfaces	328 surfaces	658 surfaces
<b>Average Magnitude</b>	0.047	0.046	0.047
<b>Median</b>	0.044	0.043	0.046
<b>RMSE</b>	0.046	0.046	0.046
<b>Standard Deviation (1σ)</b>	0.008	0.009	0.008
<b>2σ</b>	0.016	0.017	0.015

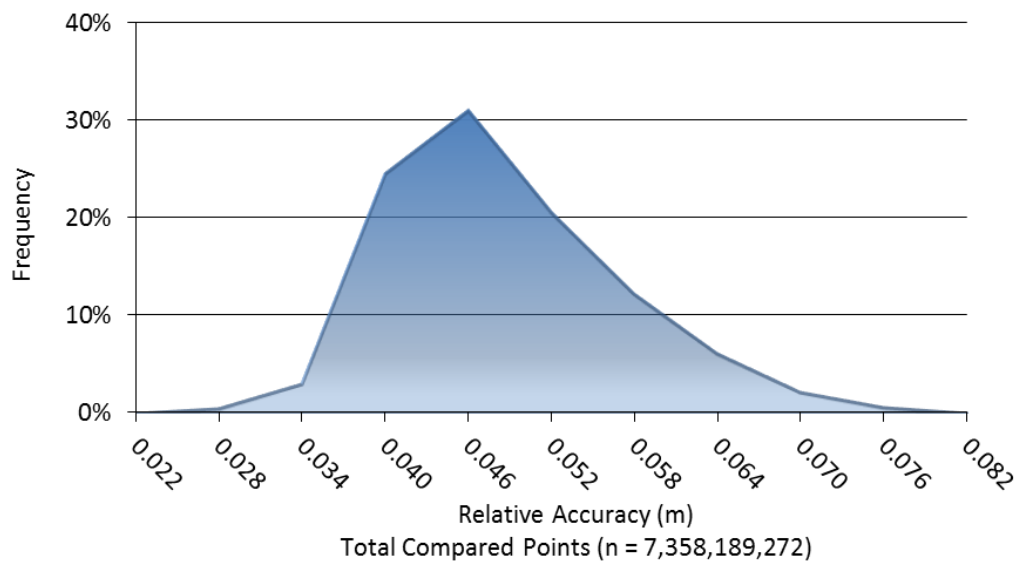


**Figure 10: Cumulative frequency plot for relative vertical accuracy between flight lines**

## Digital Imagery Accuracy Assessment

Image accuracy is measured by both air target locations and independent ground check points. Air target GPS points were measured against the placement of the air target in the imagery (Figure 2). In addition, ground check points were identified on the LiDAR intensity images in areas of clear visibility. Once the ground check points were identified in the intensity images the exact spot was identified in the orthophotography and the displacement was recorded for further statistical analysis.

The circular standard error (CSE) for the Lassen-Plumas LiDAR site was 0.35 meters. Circular standard error was approximated based on the FGDC National Standard for Spatial Data Accuracy for horizontal accuracy<sup>3</sup>. The CSE (at 39.35% confidence) was computed as follows:

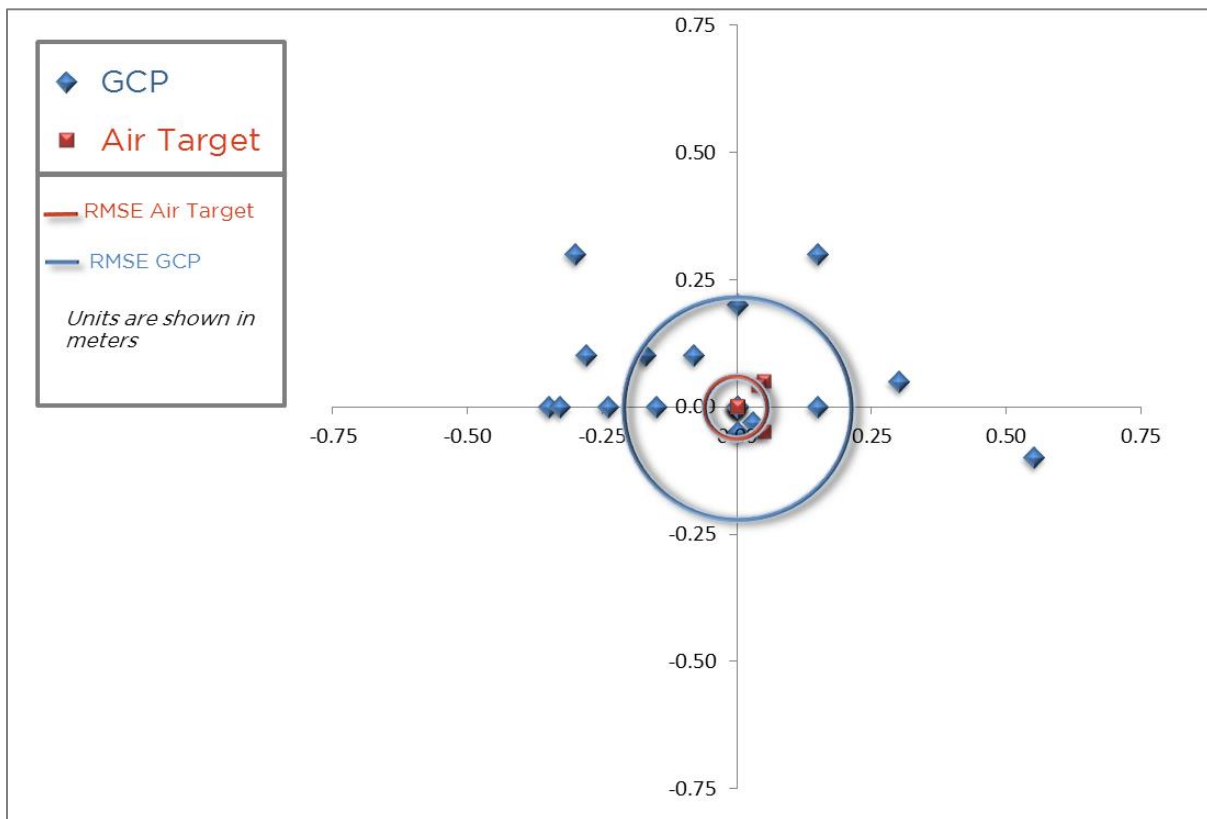
$$\begin{aligned}
 &\text{where } RMSE_x = RMSE_y; & CSE &= 1.7308 * RMSE_{xy} \\
 &\text{where } RMSE_{min}/RMSE_{max} \text{ is between } 0.6-1.0; & CSE &= 0.5 * (RMSE_x + RMSE_y) \\
 &\text{where } RMSE_{min}/RMSE_{max} \text{ is not between } 0.6-1.0; & CSE &= 2.4477 * 0.5 * (RMSE_x + RMSE_y) \\
 &(RMSE_{min}/RMSE_{max} \text{ is the lower/higher value of } RMSE_x \text{ or } RMSE_y)
 \end{aligned}$$

Table 15 presents the complete photo accuracy statistics, Figure 11 contains a scatterplot showing congruence between LiDAR intensity images and orthophotos in aerial target locations, and Figure 12 shows an example of the co-registration of the orthophotos to the LiDAR intensity images.

<sup>3</sup> Federal Geographic Data Committee, Geospatial Positioning Accuracy Standards (FGDC-STD-007.3-1998). Part 3: National Standard for Spatial Data Accuracy, Appendix 3-A, page 3-10. <http://www.fgdc.gov/standards/projects/FGDC-standards-projects/accuracy/part3/chapter3>

**Table 15: Orthophotography accuracy statistics for Lassen & Plumas National Forests**

Lassen-Plumas Photo Accuracy							
		Check Points <sub>x</sub>	Check Points <sub>y</sub>	Check Points <sub>xy</sub>	Air Targets <sub>x</sub>	Air Targets <sub>y</sub>	Air Targets <sub>xy</sub>
Count		21			7		
Mean	<i>m</i>	-0.034	0.046	0.058	0.020	0.006	0.021
RMSE	<i>m</i>	0.213	0.113	0.241	0.031	0.031	0.043
1 $\sigma$	<i>m</i>	0.216	0.105	0.240	0.015	0.023	0.028
1.96 $\sigma$	<i>m</i>	0.422	0.206	0.470	0.029	0.045	0.055



**Figure 11: Scatterplot displaying the XY deviation of aerial targets aligned with the orthophoto imagery when compared against the LiDAR intensity images**

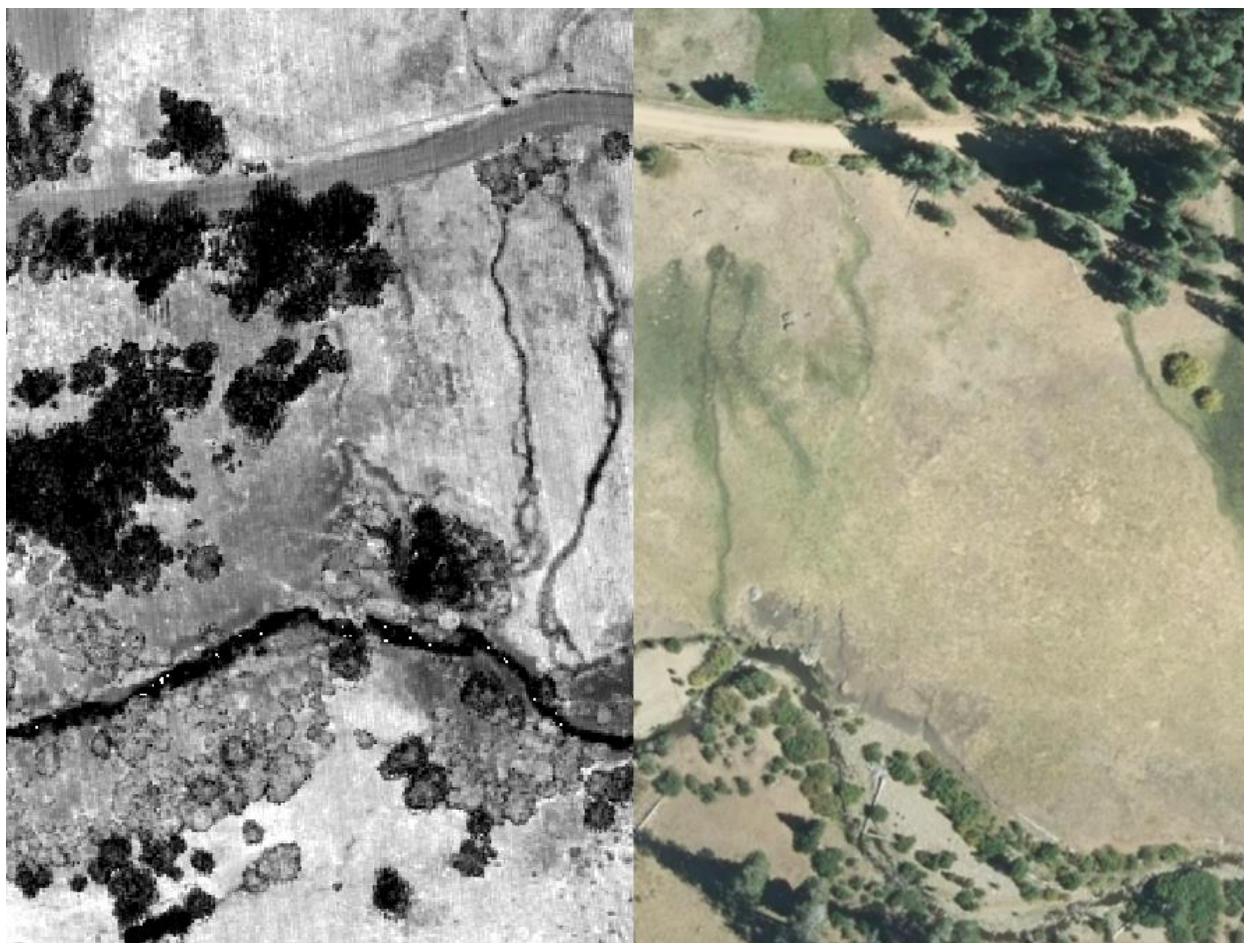


**Figure 12: Image displaying the co-registration between the LiDAR intensity image and the orthophoto at a location within the Lassen & Plumas National Forests site.**



## CERTIFICATIONS

WSI provided LiDAR services for the Lassen and Plumas National Forest study areas as described in this report.

I, Russ Faux, have reviewed the attached report for completeness and hereby state that it is a complete and accurate report of this project.

---

Russ Faux  
Principal  
WSI

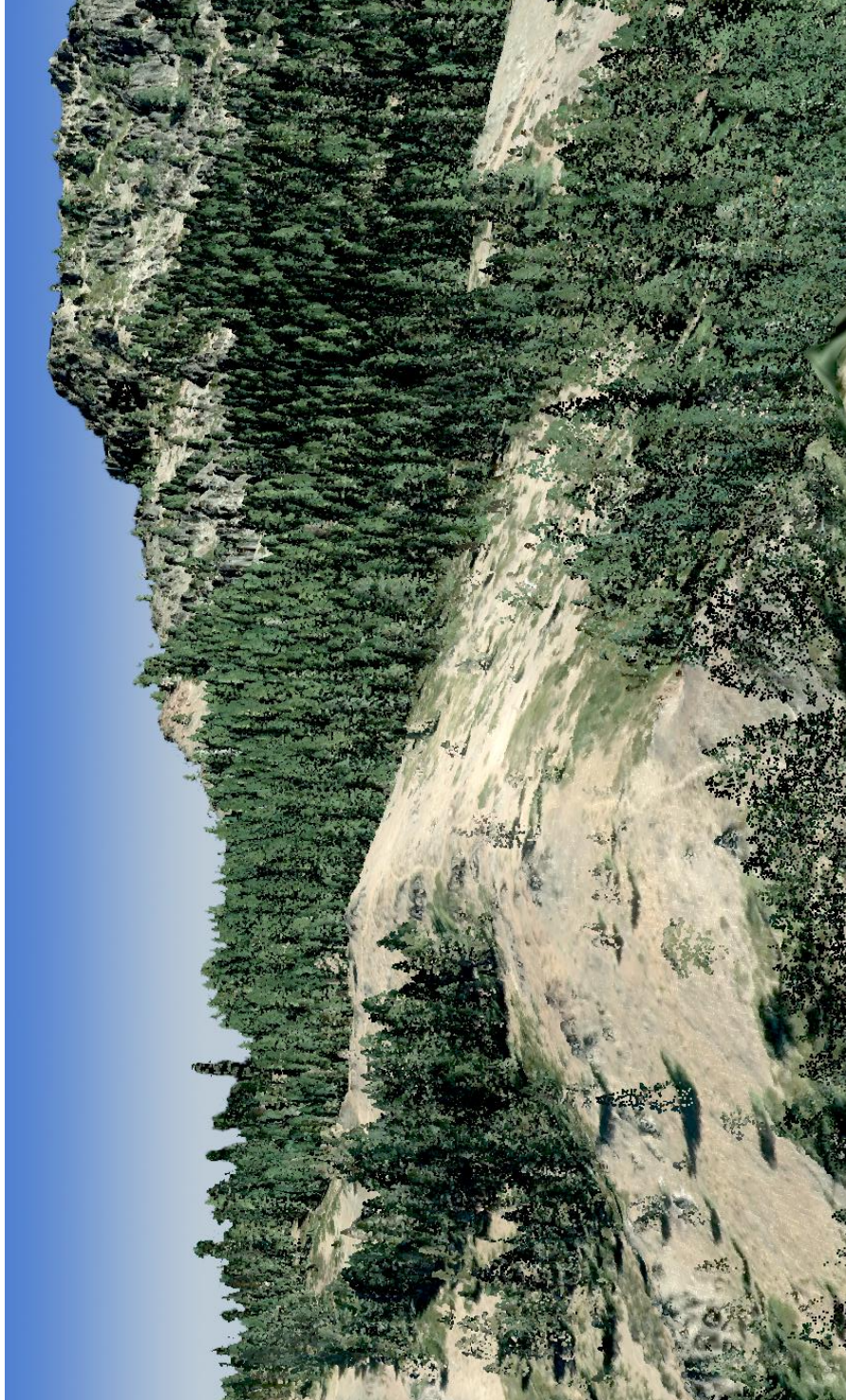


**Figure 13: View looking north towards Eagle Rocks from the Pacific Crest Trail in the Lassen National Forest.  
Image created from the LiDAR point cloud with RGB values assigned by true-color orthoimagery.**





**Figure 14: View looking north towards Wheeler Peak in the Plumas National Forest. Image created from bare-earth model colored by elevation.**



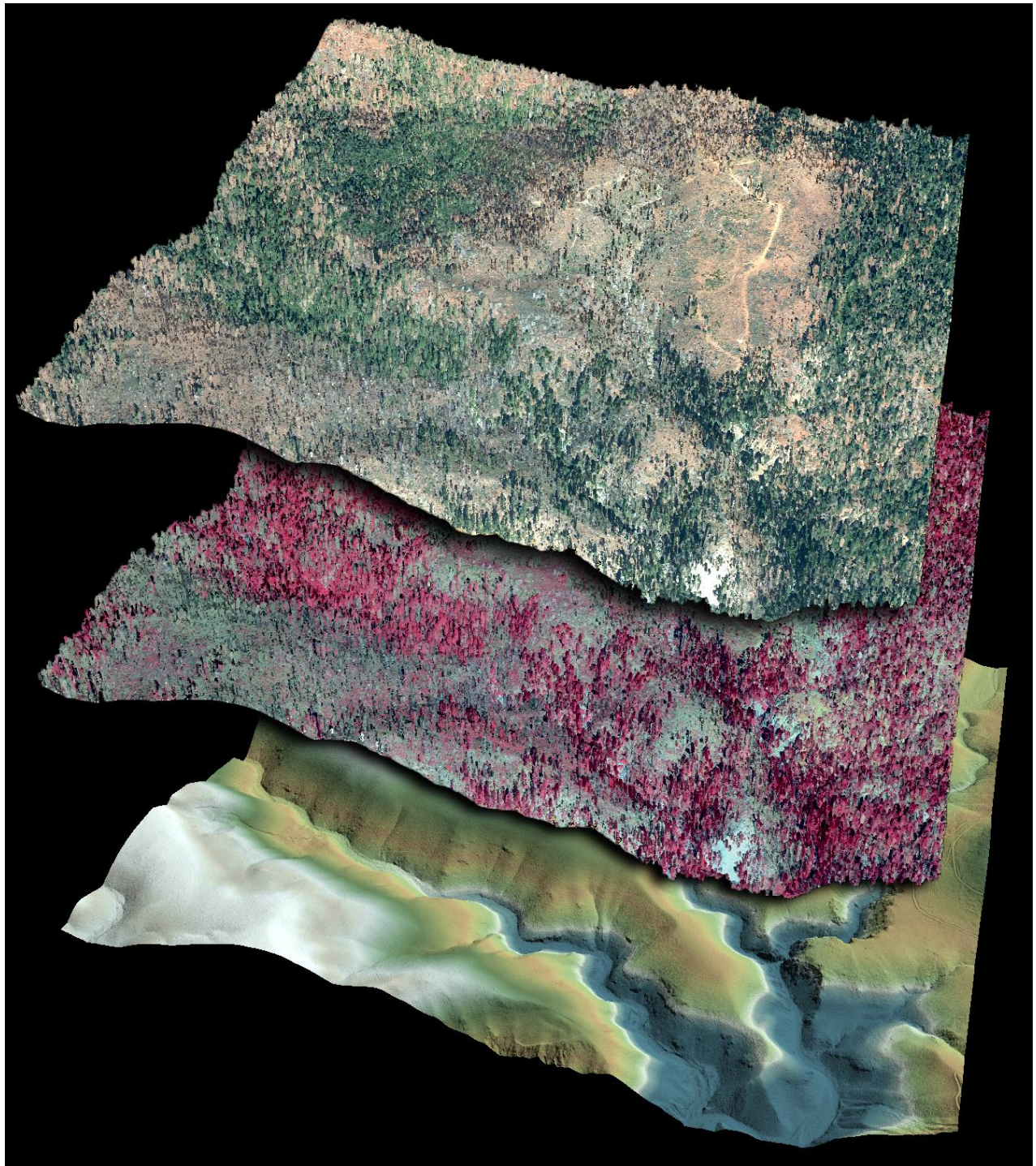
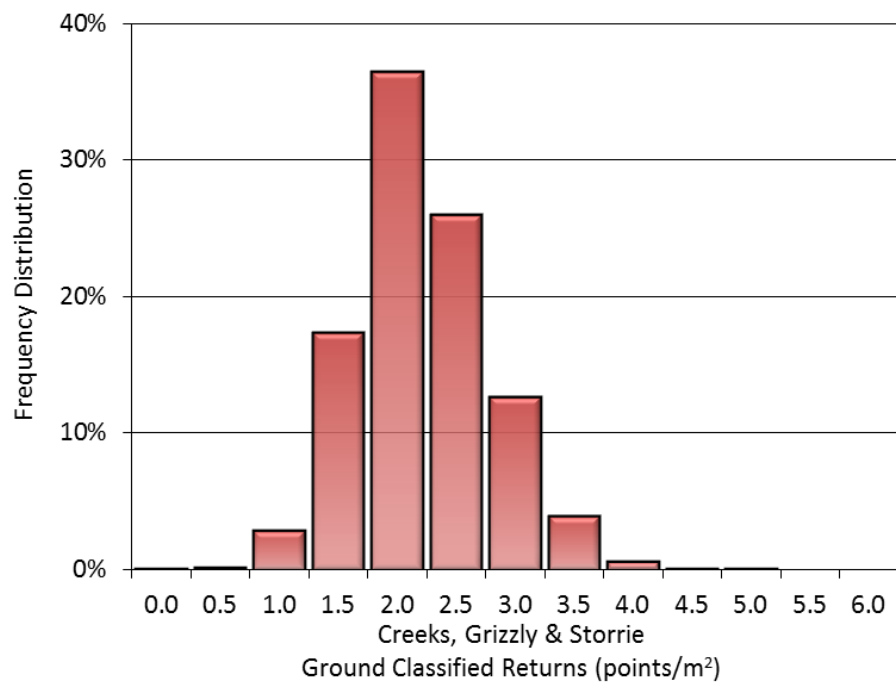
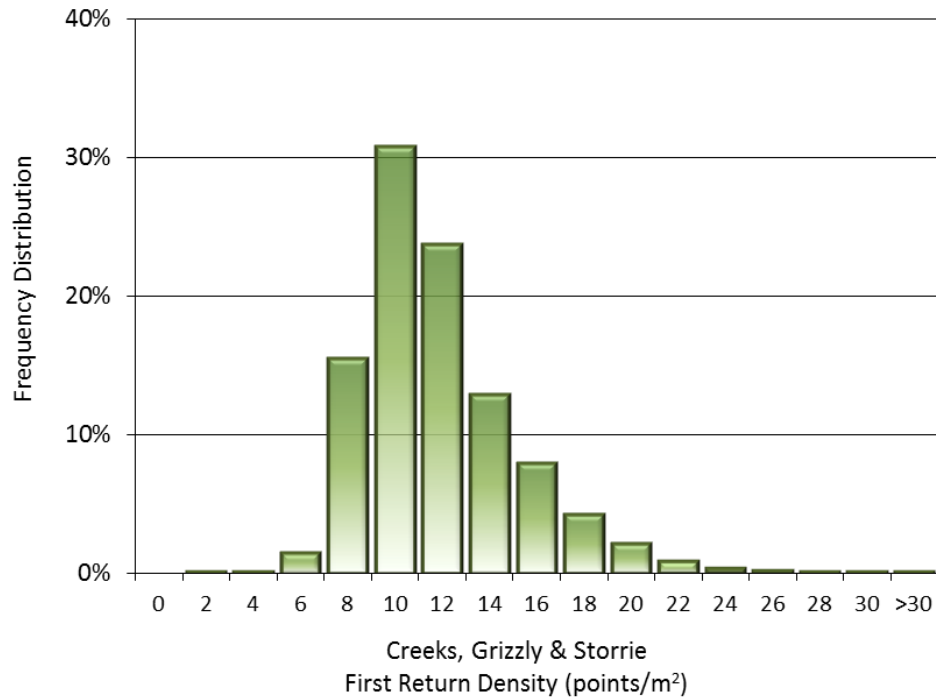


**Figure 15: Images depict a recently burned section of Grizzly Creek near Middle Campsite in the Lassen National Forest. The images were created from the LiDAR point cloud with RGB values assigned with true-color orthoimagery (top) and NIR imagery (middle). The Bottom image shows the bare-earth model colored by elevation.**

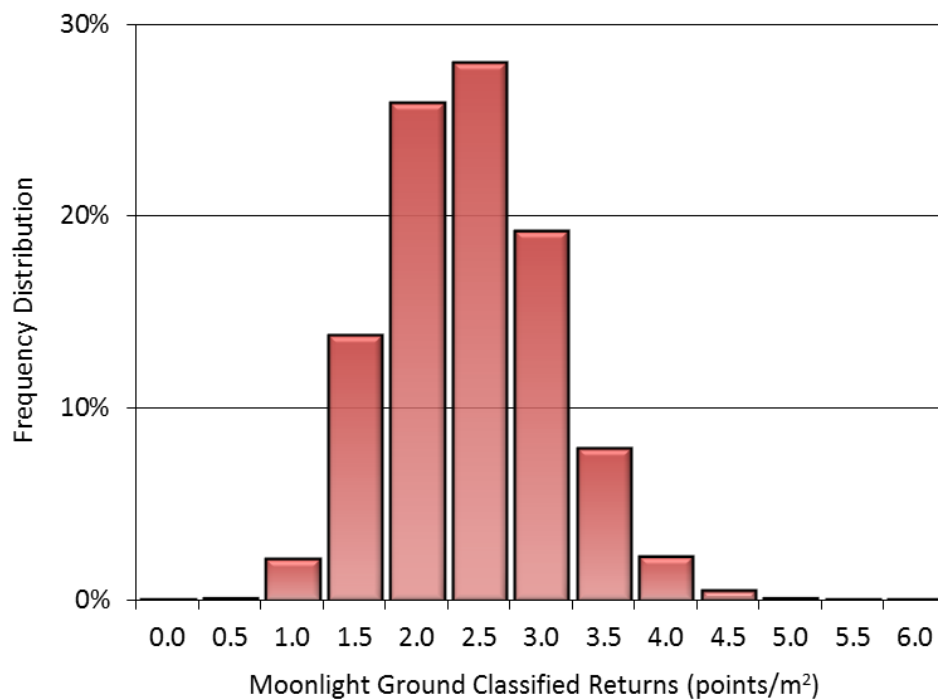
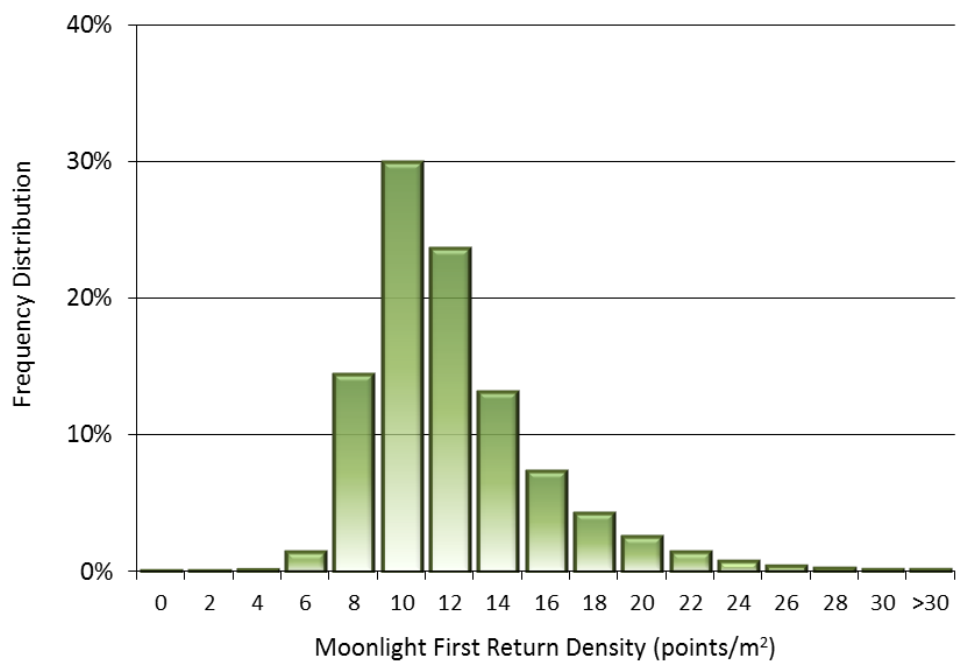


## APPENDIX A – POINT DENSITIES

Creeks, Grizzly & Storrie Frequency Distributions

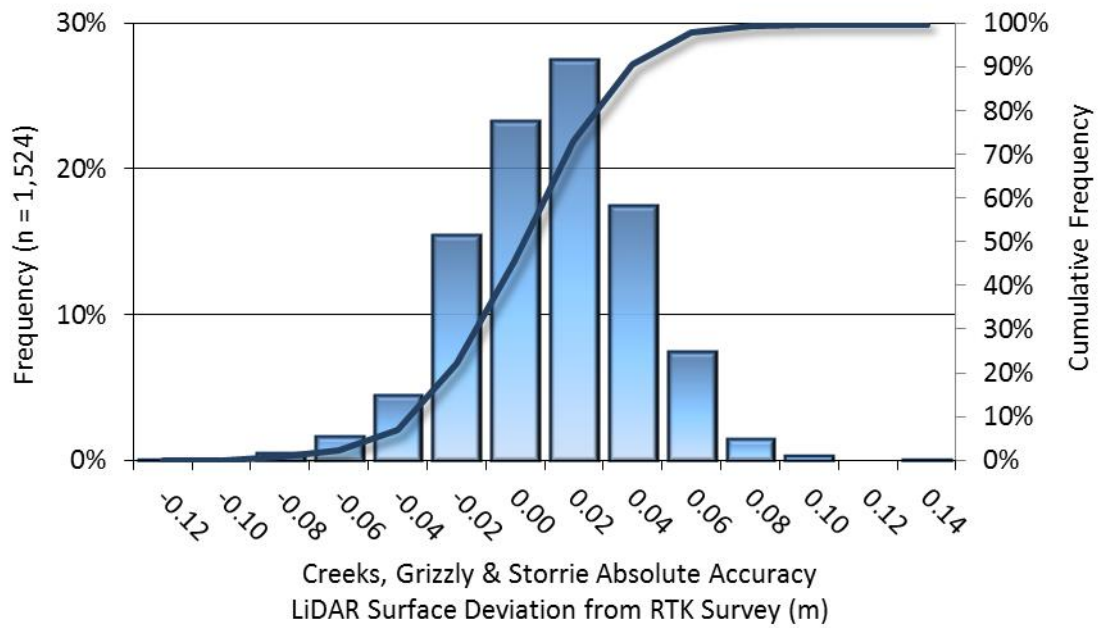


### Moonlight Frequency Distributions

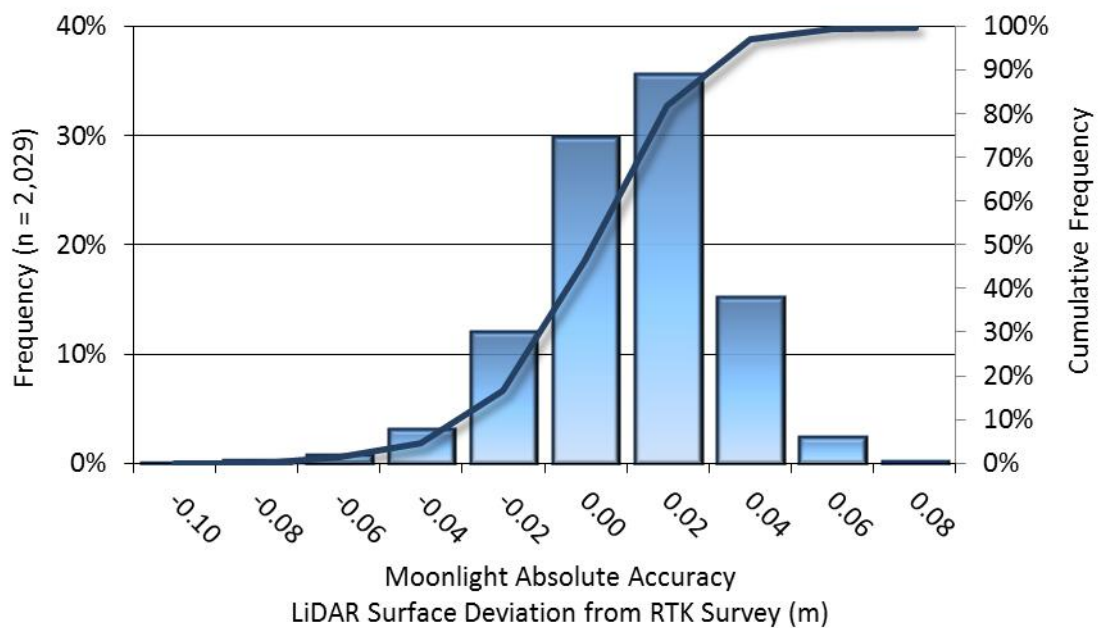


## APPENDIX B – ABSOLUTE ACCURACY

### Creeks, Grizzly & Storrie AOI

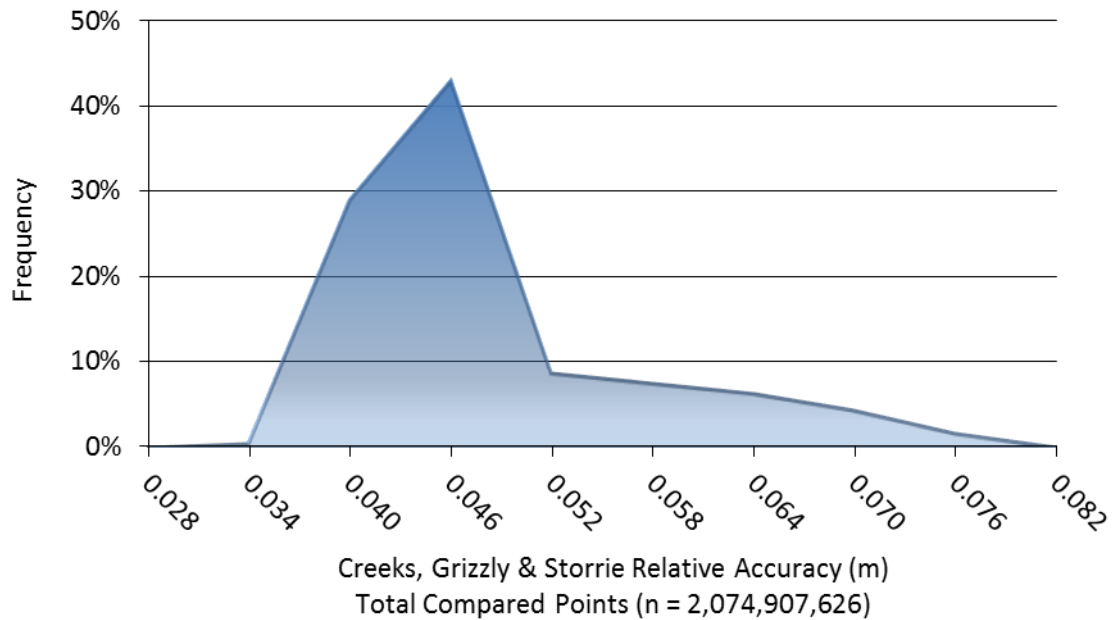


### Moonlight AOI

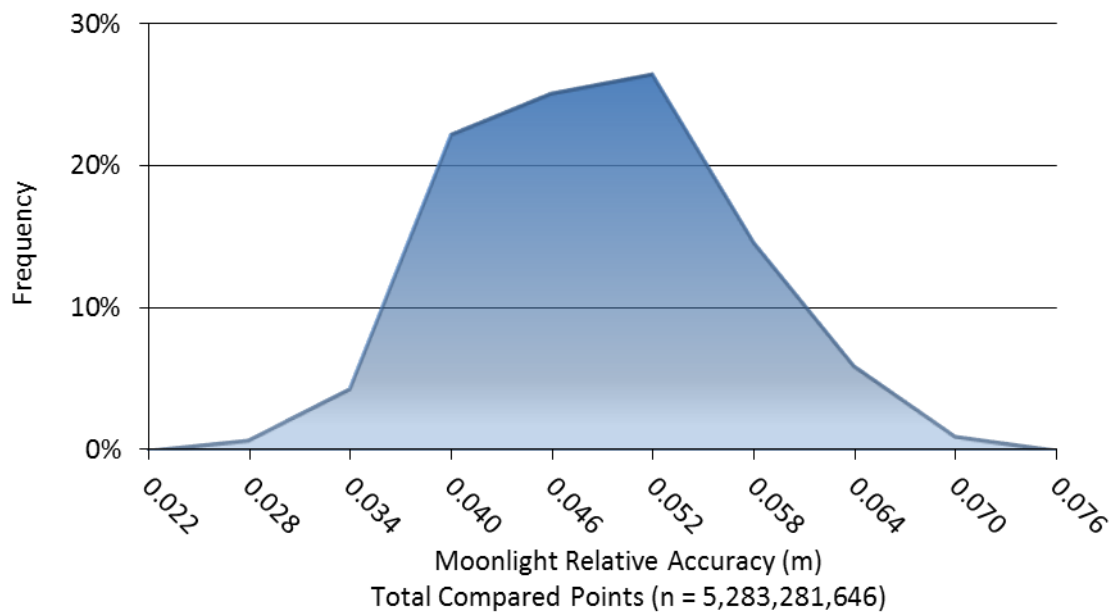


## APPENDIX C – RELATIVE ACCURACY

### Creeks, Grizzly & Storrie AOI



### Moonlight AOI





## APPENDIX D – CORS REFERENCE

This project established new monuments with reference to existing Continuously Operating Reference Stations (CORS) using the OPUS service provided by NGS (<http://www.ngs.noaa.gov/OPUS/>). The following table provides the unique four-letter identifier and positions for all CORS stations used for this project.

**CORS identifiers and published positions for this project's CORS network. Coordinates are on NAD83(2011)(Epoch 2010.00). Retrieved 10/17/2013.**

Site	Latitude	Longitude	Ellipsoid Height
CHO6	39° 25' 58.35671"	121° 39' 53.53127"	17.667
ORVB	39° 33' 16.64463"	121° 30' 00.99451"	340.571
P148	40° 25' 06.90272"	120° 48' 21.40653"	1585.055
P149	39° 36' 07.65359"	120° 06' 17.85641"	2635.233
P151	40° 17' 20.03121"	120° 04' 38.09469"	1313.586
P336	39° 31' 41.07489"	122° 25' 49.68757"	287.214
P344	39° 55' 44.82982"	122° 01' 40.64393"	50.259
P345	40° 16' 16.43056"	122° 16' 14.84864"	134.563
P346	39° 47' 40.94156"	120° 52' 02.81644"	2037.864
P349	40° 43' 51.89420"	122° 19' 09.60928"	275.864
QUIN	39° 58' 28.38082"	120° 56' 39.88941"	1106.344
RNO1	39° 32' 16.45296"	119° 53' 08.88188"	1531.180
SHIN	40° 35' 30.02899"	120° 13' 30.10386"	1377.936
STEA	39° 37' 31.94118"	119° 53' 01.17225"	1534.763
SUTB	39° 12' 20.99675"	121° 49' 14.10393"	617.102
ZOLE	39° 25' 17.99978"	119° 45' 12.03601"	1357.828

**1-sigma ( $\sigma$ ) Absolute Deviation:** Value for which the data are within one standard deviation (approximately 68<sup>th</sup> percentile) of a normally distributed data set.

**1.96-sigma ( $\sigma$ ) Absolute Deviation:** Value for which the data are within two standard deviations (approximately 95<sup>th</sup> percentile) of a normally distributed data set.

**Accuracy:** The statistical comparison between known (surveyed) points and laser points. Typically measured as the standard deviation (sigma  $\sigma$ ) and root mean square error (RMSE).

**Absolute Accuracy:** The vertical accuracy of LiDAR data is described as the mean and standard deviation (sigma  $\sigma$ ) of divergence of LiDAR point coordinates from RTK ground survey point coordinates. To provide a sense of the model predictive power of the dataset, the root mean square error (RMSE) for vertical accuracy is also provided. These statistics assume the error distributions for x, y, and z are normally distributed, thus we also consider the skew and kurtosis of distributions when evaluating error statistics.

**Relative Accuracy:** Relative accuracy refers to the internal consistency of the data set - the ability to place a laser point in the same location over multiple flight lines, GPS conditions, and aircraft attitudes. Affected by system attitude offsets, scale, and GPS/IMU drift, internal consistency is measured as the divergence between points from different flight lines within an overlapping area. Divergence is most apparent when flight lines are opposing. When the LiDAR system is well calibrated, the line-to-line divergence is low (<10 cm).

**Root Mean Square Error (RMSE):** A statistic used to approximate the difference between real-world points and the LiDAR points. It is calculated by squaring all the values, then taking the average of the squares and taking the square root of the average.

**Data Density:** A common measure of LiDAR resolution, measured as points per square meter.

**DTM / DEM:** These often-interchanged terms refer to models made from laser points. The digital elevation model (DEM) refers to all surfaces, including bare ground and vegetation, while the digital terrain model (DTM) refers only to those points classified as ground.

**Intensity Values:** The peak power ratio of the laser return to the emitted laser. It is a function of surface reflectivity.

**Laser Noise:** For any given target, laser noise is the breadth of the data cloud per laser return (i.e., last, first, etc.). Lower intensity surfaces (roads, rooftops, still/calm water) experience higher laser noise.

**Nadir:** A single point or locus of points on the surface of the earth directly below a sensor as it progresses along its flight line.

**Overlap:** The area shared between flight lines, typically measured in percent; 100% overlap is essential to ensure complete coverage and reduce laser shadows.

**Pulse Rate (PR):** The rate at which laser pulses are emitted from the sensor; typically measured as thousands of pulses per second (kHz).

**Pulse Returns:** For every laser pulse emitted, the Leica ALS 60 system can record *up to four* wave forms reflected back to the sensor. Portions of the wave form that return earliest are the highest element in multi-tiered surfaces such as vegetation. Portions of the wave form that return last are the lowest element in multi-tiered surfaces.

**Real-Time Kinematic (RTK) Survey:** GPS surveying is conducted with a GPS base station deployed over a known monument with a radio connection to a GPS rover. Both the base station and rover receive differential GPS data and the baseline correction is solved between the two. This type of ground survey is accurate to 1.5 cm or less.

**Scan Angle:** The angle from nadir to the edge of the scan, measured in degrees. Laser point accuracy typically decreases as scan angles increase.

**Spot Spacing:** Also a measure of LiDAR resolution, measured as the average distance between laser points.

## ACCURACY CONTROLS

### Relative Accuracy Calibration Methodology:

**Manual System Calibration:** Calibration procedures for each mission require solving geometric relationships that relate measured swath-to-swath deviations to misalignments of system attitude parameters. Corrected scale, pitch, roll and heading offsets were calculated and applied to resolve misalignments. The raw divergence between lines was computed after the manual calibration was completed and reported for each survey area.

**Automated Attitude Calibration:** All data were tested and calibrated using TerraMatch automated sampling routines. Ground points were classified for each individual flight line and used for line-to-line testing. System misalignment offsets (pitch, roll and heading) and scale were solved for each individual mission and applied to respective mission datasets. The data from each mission were then blended when imported together to form the entire area of interest.

**Automated Z Calibration:** Ground points per line were used to calculate the vertical divergence between lines caused by vertical GPS drift. Automated Z calibration was the final step employed for relative accuracy calibration.

### LiDAR accuracy error sources and solutions:

Type of Error	Source	Post Processing Solution
GPS (Static/Kinematic)	Long Base Lines	None
	Poor Satellite Constellation	None
	Poor Antenna Visibility	Reduce Visibility Mask
Relative Accuracy	Poor System Calibration	Recalibrate IMU and sensor offsets/settings
	Inaccurate System	None
Laser Noise	Poor Laser Timing	None
	Poor Laser Reception	None
	Poor Laser Power	None
	Irregular Laser Shape	None
		None

### Operational measures taken to improve relative accuracy:

**Low Flight Altitude:** Terrain following is employed to maintain a constant above ground level (AGL). Laser horizontal errors are a function of flight altitude above ground (i.e.,  $\sim 1/3000^{\text{th}}$  AGL flight altitude).

**Focus Laser Power at narrow beam footprint:** A laser return must be received by the system above a power threshold to accurately record a measurement. The strength of the laser return is a function of laser emission power, laser footprint, flight altitude and the reflectivity of the target. While surface reflectivity cannot be controlled, laser power can be increased and low flight altitudes can be maintained.

**Reduced Scan Angle:** Edge-of-scan data can become inaccurate. The scan angle was reduced to a maximum of  $\pm 15^{\circ}$  from nadir, creating a narrow swath width and greatly reducing laser shadows from trees and buildings.

**Quality GPS:** Flights took place during optimal GPS conditions (e.g., 6 or more satellites and PDOP [Position Dilution of Precision] less than 3.0). Before each flight, the PDOP was determined for the survey day. During all flight times, a dual frequency DGPS base station recording at 1-second epochs was utilized and a maximum baseline length between the aircraft and the control points was less than 19 km (11.5 miles) at all times.

**Ground Survey:** Ground survey point accuracy (i.e.  $< 1.5$  cm RMSE) occurs during optimal PDOP ranges and targets a minimal baseline distance of 4 miles between GPS rover and base. Robust statistics are, in part, a function of sample size (n) and distribution. Ground survey RTK points are distributed to the extent possible throughout multiple flight lines and across the survey area.

**50% Side-Lap (100% Overlap):** Overlapping areas are optimized for relative accuracy testing. Laser shadowing is minimized to help increase target acquisition from multiple scan angles. Ideally, with a 50% side-lap, the most nadir portion of one flight line coincides with the edge (least nadir) portion of overlapping flight lines. A minimum of 50% side-lap with terrain-followed acquisition prevents data gaps.

**Opposing Flight Lines:** All overlapping flight lines are opposing. Pitch, roll and heading errors are amplified by a factor of two relative to the adjacent flight line(s), making misalignments easier to detect and resolve.